EVALUATION OF HEALING IN ASPHALT BINDERS USING DYNAMIC SHEAR RHEOMETER AND MOLECULAR MODELING TECHNIQUES

A Thesis

by

RAMAMOHAN REDDY BOMMAVARAM

Submitted to the Office of Graduate Studies of
Texas A&M University
in partial fulfillment of the requirements for the degree of

MASTER OF SCIENCE

August 2008

Major Subject: Civil Engineering

EVALUATION OF HEALING IN ASPHALT BINDERS USING DYNAMIC SHEAR RHEOMETER AND MOLECULAR MODELING TECHNIQUES

A Thesis

by

RAMAMOHAN REDDY BOMMAVARAM

Submitted to the Office of Graduate Studies of
Texas A&M University
in partial fulfillment of the requirements for the degree of

MASTER OF SCIENCE

Approved by:

Chair of Committee,	Dallas Little
Committee Members,	Amit Bhasin
	Charles Glover
	Eyad Masad
Head of Department,	David Rosowsky

August 2008

Major Subject: Civil Engineering

ABSTRACT

Evaluation of Healing in Asphalt Binders Using Dynamic Shear Rheometer and Molecular Modeling Techniques. (August 2008)

Ramamohan Reddy Bommavaram, B.Tech., Indian Institute of Technology - Madras

Chair of Advisory Committee: Dr. Dallas Little

A self-healing material has the inherent ability to partially reverse damage such as crack formation that might have occurred during its service. Significant evidence exists in the literature to indicate that asphalt binder is a self-healing material. It is also well known that healing has a substantial affect on the performance of asphalt mixtures and consequently on the serviceable life of asphalt pavements. For example, shift factors from laboratory experimental data to field observed data show that laboratory data under-predict field observations. There is a need to understand the mechanisms that are responsible for healing in asphalt binders as well as to develop test methods that can be used to determine properties related to these mechanisms. This thesis presents details and findings from a two-part study that addresses each one of these two aspects. In the first part of this study, a test method based on the use of a Dynamic Shear Rheometer (DSR) was developed to determine the parameters of characteristic healing function of asphalt binders. In the second part of this study, Molecular Modeling (MM) techniques were used to determine the interrelationship between molecular structure, surface free energy, self diffusivity, and other healing properties of asphalt binders.

The healing characteristic equation parameter (Ro) which represents the instantaneous healing nature of the asphalt binders is analogous to surface energy in terms of effect on healing in asphalt binders. Ro values for three asphalt binders AAM, AAD and ABD are calculated and compared with the surface energy values available from the literature. It was observed that the Ro values are proportional to surface energy values. Surface energy values for five asphalt binders AAM, AAD, AAB, AAG and AAF are calculated using MM method based on SHRP representative molecules. These values were observed to be proportional to the surface energy values from literature. Bulk and surface diffusion coefficients of asphalt molecules are calculated using MM method. Parametric analysis was done to determine the effect of chemical structure of asphalt on its diffusion properties. It was observed that the higher percentage of saturates in the chemical structure results into higher diffusion coefficients.

To my Mother and Father...

ACKNOWLEDGEMENTS

I take this opportunity to thank my chief advisor, Dr. Dallas Little, for his encouragement, guidance and support throughout my entire graduate studies. I also would like to thank Dr. Amit Bhasin for his invaluable support. This thesis would not have been possible without his vision and direction. I am very fortunate for having the opportunity to work with these two people and I will cherish these memories for my entire life.

I wish to express my sincere thanks to Dr. Eyad Masad and Dr. Roger Smith for their suggestions and guidance throughout my graduate studies. I also would like to thank Dr. Charles Glover, Dr. Greenfield and Dr. Lisa M Perez for their valuable inputs towards my research on molecular modeling analysis. In addition, my special thanks to Dr. Murali Krishnan for his invaluable support, encouragement and inspiration.

This thesis would not have been possible without the constant support and encouragement of my friends: Chidvilas, Prasad, Raghudeep, Ravi, Srikanth and Kiran. Along with them I also would like to thank my friends Jyothirmoy, Karthik, Rajesh and many others who made my stay at A&M a wonderful experience.

Finally, I would like to thank my family for their constant encouragement and love throughout my academic career.

TABLE OF CONTENTS

Page

Page

LIST OF FIGURES

Page

Page

1. INTRODUCTION AND SIGNIFICANCE OF THE RESEARCH

Nations from all over the world are continually trying to discover and extract crude oil from new sources. As a result, there is a high variability in the physical and chemical properties of crude oil and even higher variability in the residue after distillation such as asphalt binder. Owing to the high variability and extremely complex physical and chemical nature of asphalt binders, it is challenging for the pavement and transportation industry to accurately predict the performance of flexible pavements that utilize these binders. Although considerable improvements in the characterization of asphalt binders and performance prediction of asphalt mixtures have been achieved in last two decades, there are still several challenges that need to be addressed. One such challenge is being able to accurately understand and quantify the role of self healing in asphalt binders and mixtures.

More than ninety percent of the road network in United States is comprised of flexible pavements. Asphalt mixture, a composite of asphalt binder and aggregate, is the key material that is used in the construction of a flexible pavement. Asphalt binder maintains the integrity of the asphalt mixture by gluing the aggregates and filler particles together. Thus, the performance of a flexible pavement largely depends on the behavior and performance of the asphalt mixture composite.

This thesis follows the style of *Transportation Research Record*.

The performance of an asphalt mixture can be assessed based on its resistance to various modes of distress such as fatigue cracking, permanent deformation, and moisture damage. One of the important factors that dictate the resistance of an asphalt mixture to fatigue cracking is the healing characteristic of the asphalt binder. Healing, in this context, can be briefly defined as the process by which the crack growth in asphalt binders or mixtures, which occurs due to repeated loading, is partially or completely reversed. For example, cracks may develop in an asphalt mixture due to the repeated loads from passage of vehicles. However, if the pavement is allowed to remain without any external load or vehicles for sufficient time, these cracks can reverse on their own due to the self healing nature of the asphalt binders. Thus, understanding the healing characteristics of asphalt binders allows us to optimize the use of asphalt mixtures in an economical way.

Although, there is a general consensus that healing in asphalt binder has a significant impact on the performance of asphalt mixtures, there is very limited work done to fully understand and quantify the intrinsic healing mechanism of asphalt binders. Most of the laboratory tests conducted using asphalt binders or composites provide an ad-hoc comparison of the healing characteristics for different materials. Typically, healing in an asphalt composite is quantified by subjecting the test specimen to some form of cyclic loading and then determining the relative increase in performance (such as dissipated pseudo strain energy) before and after a rest period in between the load cycles. The results from such tests are extremely useful to provide evidence of healing and relative ranking of the propensity for different materials to heal. However, the

disadvantage is that these tests are highly dependent on the nature of the applied load, duration of rest period, and intervals between load cycles in which the rest period is provided. Consequently, the results from these tests cannot be used directly to model the performance of asphalt pavement structures that are subjected to different loading and environmental conditions. In order to better relate the laboratory test results to the field performance, it is important to understand the mechanism of self healing in asphalt binders as well as develop a simple test method to determine the intrinsic healing characteristics of different asphalt binders. Given the complex physical and chemical composition of asphalt binders, it is unlikely that a single parameter can be used to describe and quantify the healing in binders. This research comprises of two major tasks. The first was to develop a simple test method to determine the intrinsic rate of healing of an asphalt binder. The intrinsic rate of healing or intrinsic healing function, R(t), may be simply defined as the relationship between gain of strength of two completely wetted crack surfaces as a percentage of strength of the virgin material over time. In this study, a test method using the Dynamic Shear Rheometer (DSR) was developed in order to determine the intrinsic healing function for different asphalt binders. In the second part of this research, molecular modeling techniques were used to determine the relationship between molecular morphology, surface energy, self diffusion coefficients, and self healing characteristics of different asphalt binders.

A brief introduction of the hypothesized healing mechanism and research approach is as follows. The general basis for the healing mechanism is similar to the model proposed by Wool and O'Connor *(1).* When the two surfaces of an asphalt binder

come into contact, as in the case of a crack that closes, they tend to heal or regain strength with respect to time. The process of the cracked surfaces coming into contact with each other is referred to as *wetting*. The rate of wetting is influenced by the mechanical properties of the material as well its surface free energy. At the time when a given region is completely wet, t = 0, there is an instantaneous, but limited, strength gain for the wetted portion of the crack due to the interfacial work of cohesion between the crack surfaces. The work of cohesion of the asphalt is also dependent on its surface free energy. With passage of time, the interfacial strength across the original crack surface gradually increases. At sufficiently longer time the strength across the original crack surface can theoretically reach that of the virgin binder i.e. $R(\infty) = 100$ %. This increase in strength across a wetted crack interface over time can be considered as an intrinsic property of the asphalt binder and is governed by the self diffusivity of its constituent molecules. The strength gain across the crack interface is also reflected in the mechanical properties of the material. For example, the shear modulus of an asphalt binder across a cracked surface can be monitored over time to determine the intrinsic healing function.

As described above, surface free energy and self diffusion coefficient are the two important properties of the asphalt binder that govern its characteristics. Surface free energy is an important parameter in the rate of wetting and the initial strength gain where as the diffusion properties define the long term healing nature. Sophisticated molecular modeling techniques can be used to determine the role of molecular morphology on the surface free energy and diffusion properties of asphalt binders and consequently on the

rate of healing. One limitation in this regards is that it's the exact chemical composition of asphalt binders is highly complex and variable depending on the source of the crude oil. In view of this limitation, in this research, molecular modeling can be used to conduct a parametric analysis of the impact of changes in molecular morphology on the properties related to healing (surface free energy and self diffusion coefficient) rather than determining the absolute values for these properties.

This thesis is divided into five sections. This first section is to provide a brief introduction about the need and objectives of the research. The second section provides further details and a summary from the literature review that is relevant to both aspects of this research, i.e. i) use of a DSR to determine the intrinsic healing function of asphalt binder, and ii) use of molecular modeling techniques to determine the properties of asphalt binder related to healing. The third and fourth sections present the development of the DSR based test method and the use of molecular modeling techniques to determine properties related to healing in asphalt binders, respectively. Each of these sections is further divided into subsections on the back ground of the test method or technique, procedure used, results and findings. Section five presents the pertinent conclusions from the research work and scope for future work.

2. LITERATURE REVIEW

Due to the importance of crack healing in asphalt materials and its consequent effect on the performance of flexible pavement, many researchers have tried to incorporate the effect of healing in their experimental work since late 1980's. Most of the significant work done in this area can be dated to very recent years. Research on the area of healing in asphalt materials can be divided into two broad categories. The first category is research related to quantifying the effect of healing on the performance of asphalt mixtures. The second category is research related to understanding the mechanisms of healing and the material properties that contribute to macroscopic healing in asphalt materials. Of course, research in both these areas is highly interrelated. Accordingly, the two main objectives of this research are i) to develop a method using the DSR to determine the intrinsic healing function of an asphalt binder, and ii) to evaluate the effect of molecular morphology of asphalt binders on properties related to healing. This section is divided into two subsections. The first subsection briefly explains the earlier work done in the area of evaluating the healing characteristics of asphalt binders using mechanical properties. The other subsection concentrates on previous work related to the use of molecular modeling techniques.

2.1 Literature Review Related to Quantification of Healing in Asphalt Mixtures

Some of the most recent, significant documentation of healing in the laboratory was demonstrated by Little et al. *(2)*, by Kim et al. *(3)*, by Carpenter and Shen *(4)* by Kim and Roque *(5),* and by Maillard et al. *(6).* Data from these laboratory studies clearly

demonstrate the evidence for existence of healing and its significant impact on the fatigue cracking life of asphalt mixtures. Little et al (*2)* demonstrated that rest periods (of 24-hour duration) applied in traditional flexural beam bending experiments increased the fatigue life by more than 100 percent depending on the type of binder used. Kim et al. *(3)* used torsional loading on asphalt mastics to demonstrate that rest periods of between 30-seconds and 2-minutes extend fatigue life and decrease the rate of accumulation of the dissipated energy that actually causes damage (measured as pseudo strain energy). Their work also showed that the impact of healing is by far the greatest when rest periods are applied before significant damage occurs.

Carpenter and Shen *(4)* skillfully verified this conclusion by demonstrating that the application of short rest periods between each load cycle not only extends fatigue life but is also responsible for the extension of so called "endurance limit" of some asphalt mixtures. They used dissipated energy between load cycles to quantify healing. Kim and Roque *(5)* used a similar approach to quantify the healing characteristics of asphalt binders used in different asphalt mixtures. They quantified healing in terms of the recovered dissipated creep strain energy per unit time.

Maillard et al. *(6)* conducted tensile tests on films of asphalt binders lodged between glass spheres to simulate an asphalt film that is bound by aggregates. They measured the rate of healing in the asphalt film by transmitting ultrasonic waves through the sample. A decrease in the amplitude of the ultrasonic signal corresponds to damage in the film. An increase in the amplitude of the ultrasonic signal for an undisturbed

sample after applying a tensile load corresponds to the healing process. The effect of healing during rest periods is also evidenced in the permanent deformation characteristics of asphalt mixtures. For example, Bhairampally et al. *(7)* demonstrated that the inclusion of rest periods between compressive load cycles extended the time to tertiary damage and that this extension depended on the type of asphalt. Their work concluded that the transition from the secondary phase to the tertiary phase of dynamic compressive creep is related to development and growth of micro cracks. Further work by Song et al. *(8)* has shown this to be true using computer assisted tomography. Bhairampally et al. *(7)* also demonstrated that addition of a filler (in this case hydrated lime) resulted in reduced rates of damage in the compressive mode of loading because of crack pinning and accentuated the effect of healing of micro cracks in the mastic.

In addition to laboratory evaluations, there is evidence in the literature to demonstrate the presence of healing in asphalt field pavements. Williams et al. *(9)* presented some convincing field data related to healing. They selected four pavement sections at the Turner Fairbanks accelerated load facility (ALF) considering a full factorial of two thicknesses and two asphalt layer types over a homogeneous subgrade. Surface wave measurements were made to assess pavement stiffnesses before, immediately after, and 24-hours after loading passes. Regardless of the pavement type, the trend was that more healing (quantified in terms of the recovery of stiffness) was recorded closer to the centerline suggesting that more fatigue damage results in a greater potential for and a greater amount of micro damage healing. Williams et al. *(9)* reported other convincing support for healing using surface wave analysis of pavements at

Mn/ROAD pavement sections and on U.S. Highway 70 in North Carolina using designed experiments. Nishizawa et al. *(10)* used data from four thick pavements to demonstrate that fatigue cracking did not occur because healing effects at the low strain and low damage levels compensated for (off set) crack growth. Little and Bhasin *(11)* presented a more detailed review on the evidence of healing as well as methodologies used to quantify the effect of healing on the performance of bituminous materials.

2.2 Literature Review Related to Molecular Modeling Techniques

2.2.1 Molecular Composition and Structure of Asphalt Binders

Robertson et al. *(12)* present a detailed description of the nature of molecular structure in an asphalt binder. At the molecular level, much of the total mass of a neat asphalt binder is a mixture of a wide variety of high-boiling hydrocarbons i.e. compounds containing hydrogen and carbon. Some of these hydrocarbons are aliphatic (oily or wax materials), some are aromatic, and some molecules have both aliphatic and aromatic carbon. All of the naturally occurring hetero atoms, nitrogen, sulfur, oxygen, and metals contribute to polarity, or asymmetric charges distribution, within these molecules. In general, the boiling points of polar molecules will be greater than that of similar non-polar molecules. This is because it takes more energy to separate polar molecules than to separate non-polar molecules of similar molecular size due to the higher attraction among the polar molecules in liquid state. Polarity also is the prime reason for H-bonding.

The polar molecules tend to associate strongly to form organized structures throughout the continuous phase of the relatively non-polar portion of the asphalt. Polar molecules interact with each other to form assemblages leading to the viscous nature of the asphalt. Non-Polar molecules on the other hand act as the solvent and the solvent power varies from one asphalt type to another. Oxidation has a pronounced effect on the organized structure. As oxidation occurs, new polar sites are formed in addition to those in the virgin asphalt. As a result, the propensities for molecules to self associate or self assemble increases and results in an increased stiffness. SEC – Size Exclusion Chromatography, using toluene, can be used to separate molecules by apparent molecular size. This technique is based on the assumption that if there are associated groups of molecules in the whole asphalt, they will persist in concentrated toluene solution and therefore can be separated as associated materials by SEC. Vapor-phase-osmometry, using pyridine, can be used to break up self assembled molecules. NMR is another technique used to discern the structure of asphalt molecules.

Storm et al. *(13)* demonstrated that NMR techniques could be used to generate molecular representations that automatically provide estimates of the number average molecular weight. The estimates provided by Storm et al were consistent with the upper bound of the number average molecular weight that was obtained previously for similar asphaltenes. One type of single molecular representation is generated by combining data obtained both liquid state C-13 and H NMR; the other using the data obtained with solid state C-13 NMR. The procedure and findings from NMR spectra analysis by Storm et al. *(13)* is summarized below.

For liquid state NMR spectra analysis, Proton (300 MHz) and C-13 (75 MHz) NMR spectra were measured at room temperature using a 5-mm switchable $^{1}H/^{13}C$ probe on a Varian VXR-300 spectrometer. Five chemically distinct carbon items were reported: aliphatic carbon from 10 to 60 ppm; aromatic carbon from 110 to 160 ppm; the sum of aromatic carbon shared by three rings (triple bridgehead carbon) and aromatic carbons with a hydrogen attached from 110 to 130 ppm; the sum of aromatic carbon shared by two rings, napthenic carbon, and aromatic carbon with an attached methyl group from 130 to 138 ppm; and finally aromatic carbon with an attached alkyl group from 138 to 160 ppm. Similarly various types of hydrogen atoms were also distinguished and reported based on the H NMR spectra. Representative molecules for asphaltenes based on these various carbon and hydrogen groups were reported.

Solid state 13C NMR spectra obtained at 75.44 MHz on a Varian unity-300 spectrometer, using a Doty scientific 7-mm multinuclear CPMAS probe were also reported by Storm et al. *(13).* Solid-hexa-methyl benzene was used as the standard. The reported spectra were obtained using cross polarization (CP), magic angle spinning (MAS), and high power proton decoupling. The two types of single molecule representations (obtained through solid and liquid state NMR display essentially equivalent molecular characteristics. Since they are generated by applying essentially two different analytical techniques, and both are consistent with the upper bound on molecular weight. Storm etal. *(13)* reported that that this similarity of molecular characteristics suggests that the asphaltenic molecules were much smaller than

previously assumed and that R groups attached to the poly-nuclear aromatic core are not as long as previously believed.

In this research, the molecular structures determined by Jennings et al. *(14)* for SHRP asphalt cements were used as inputs. These structures were determined based on NMR spectroscopy in solution-state and solid-state. Jennings et al. reported data were obtained on the amounts of aromatic carbon in an average molecule of the asphalt sample, the manner in which that carbon is arranged in terms of the size of the average aromatic system and the extent of substitution. The arrangement of aliphatic portion was also described in terms of the average number of alicyclic rings, of aliphatic chain length and the extent of branching. Concentrations of carboxylic acids and phenols were measured both before and after laboratory oxidative aging.

Jennings et al. *(14)* reported details about the overall chemical nature of asphalts using solution state NMR. They also reported the ability of asphalt molecules to assemble into rigid structures using solid-state NMR. Their work on solution state NMR work concentrated on three characteristics of asphalts: the aromatic portion, the aliphatic portion (including alicyclic i.e. napthenic) and chain type structures. They reported pi-pi interactions among the stacked flat aromatic systems and van der Waals interactions among aliphatic molecules with longer chains and fewer branches and polar interactions involving hetero atoms. They used these data to propose a representative molecule for each of the eight SHRP asphalts; AAC, AAM, AAD, AAK, AAG, AAA, AAB and AAF.

2.2.2 Molecular Modeling of Polymers and Thin Films

Molecular modeling is a collective term that refers to theoretical methods and computational techniques to model or mimic the behavior of molecules. Although, as of now, not much research work is done towards the molecular modeling of asphalt binders, these techniques have been widely used to model the behavior of polymers. One main limitation for the use of molecular modeling techniques to evaluate the properties of asphalt binder is the highly complex nature of its constituent molecules. With the advent of technology, advancements in determining the molecular structure of asphalt binders can result in improved accuracy and scope for the usage of molecular modeling techniques.

Deng et al. *(15)* Worked on the performance of multi-layered material systems. The performance and strength of many composites, hybrid and thin multi-layered material systems are very much dependent upon the mechanical properties of interfaces. However, continuum mechanics approach to characterize interfacial properties has limited success because it is often unable to incorporate the effects of molecular and chemical reactions into the model. At this scale, continuum mechanics breaks down and techniques for submicron experiments are still not fully developed. Molecular Dynamics (MD), simulations can provide information on interfacial strength and mechanical properties of interfacial constituents at a more fundamental level. Central to all MD calculations is the selection of an appropriate force field to describe the potential energy surface. The potential controls the motions of polymer chains because forces for molecular motion are derived from the first spatial derivatives of the potential. In

general, the force fields of polymer systems are derived from the sum of bond, cross-term and non-bond interactions.

Significant work related to molecular modeling has already been conducted in the field of polymers. Clancy and Mattice *(16)* studied the interfaces, thin faces and amorphous cells of various hydrocarbons using molecular modeling techniques. Software from Molecular Simulations, Inc (which is a part of Accelrys since 2001) was used for simulation purposes. The polymers used in their study included Polypropylene (PP), head to head polypropylene (hhPP), P78 (a random polymer composed of 22% of a linear monomer and 78% of branched monomer), polyethylene propylene (PEP), PE2P2 etc.

The procedure used by Clancy and Mattice *(16)* is briefly described in the following paragraphs. This procedure is typical for the evaluation of thin polymer films and was also used as the basis for the molecular modeling of asphalt binders (described in Section 4). Amorphous cells for each of the polymers were constructed, based on the densities available in the literature, using a procedure by which a single chain is packed into a box with periodic boundary conditions. Depending on the density and molecular weight of the polymer the edge length of the periodic boxes were varied from 18.97 A^o to 20.69 A^o. The chain was then shaken by performing NVT Molecular Dynamics at high temperatures (500 K – 1000 K) for approximately 10 ps. Snapshots of the trajectory during last half of the run were taken at every 0.05 ps. The snapshot with minimum PE is selected and minimized with a conjugate gradient minimizer to a convergence of 0.01

kcal per mole per A^o. These amorphous cells were used for two purposes, to create the thin films and also to determine the surface properties. While measuring surface properties it was to be taken care that both bulk and thin films are of same density. But the thin films created from these amorphous cells would be of lower density and hence the densities of these amorphous cells were to be readjusted. Thus, these amorphous cells were equilibrated at the density matching that of the interior of the corresponding thin film by NVT MD simulations at approximately 300 K for 50 ps. A snapshot of minimum PE is taken from the last half of the simulations and is minimized using conjugate gradient minimizer. The resulting structure is used to determine the cohesive energy and the solubility parameter using the Ewald summation technique as supplied in the Amorphous Cell software module of the MSI software.

Thin films were constructed from the amorphous cells by elongating one of the periodic boundary conditions such that the parent chain no longer interacts with its image along that coordinate. The z coordinate was extended to 100 A^o from roughly 20 A^o of the corresponding amorphous cell. The resulting thin films are subjected to MM energy minimization followed by 50 ps of MD simulation at 300 K. Snapshots of the trajectory were taken at every 0.01 ps during the last half run of the MD simulation. The snapshot of the lowest potential energy was minimized using MM energy minimization techniques. The surface tension of the resulting thin film was calculated from the difference in energy of the thin film and the energy of the corresponding amorphous cell divide by the surface area created upon formation of the thin film as given by the equation below.

$$\gamma = \frac{E_{thin\ film} - E_{amorphous\ cell}}{2A} \quad (1)$$

Interfaces were created by bringing the two thin surfaces together. The resulting thin interfacial system subjected to MM energy minimization followed by 50 ps of MD simulation at 300 K. Snapshots of the trajectory were taken at every 0.01 ps during the last half run of the MD simulation. The snapshot of the lowest potential energy is minimized using MM energy minimization techniques. The work of adhesion is calculated from the difference in energy between the interfacial system and the energy of the two separated thin films which comprise the interface. The work of adhesion, w_{12}, used from this method is then used to calculate the interfacial tension, γ_{12}, using the surface tension values obtained from the thin film simulations as given by following equation; $\gamma_{12} = \gamma_1 + \gamma_2 - w_{12}$. As expected, the interfacial tension values for the interfaces with similar polymers are almost equal to zero.

The solubility parameters were derived from the calculated cohesive energy density values. A comparison between the differences in solubility parameters among the bulk polymers in this simulation and the difference in the solubility parameters found in experiment by single angle neutron scattering (SANS) at 27 degree Celsius, is made. The total energy could be divided into two parts; local intra-molecular (which is sum of bond stretching, angle bending and torsion terms) and non bond energy (van der Waal's which can further be divided into repulsive & dispersive, and electrostatic terms). The constituent energy terms combined with the bond order parameters values are used to analyze the effect of the presence of methyl and ethyl groups and their orientation at the

surfaces on the final energy terms. The division among the energetic terms indicates that the local intra-molecular energy decreases upon formation of the thin film while the non-bond energy, consisting primarily of the van der Waals term increases. Attractive interactions were observed between some of the pairs of films. The distribution among the energetic terms of these interactions between some of the pairs of films seems to indicate that attractive interaction is brought by favorable local intermolecular energetic terms rather than simply by van der Waals interactions alone.

2.2.3 Molecular Modeling of Asphalt Binders

Some of the most significant work in the recent times that is directly related to the molecular modeling of asphalt binders can be attributed to Greenfield and co-workers. Greenfield and Zhang *(17)* used molecular simulations to estimate the properties of three-component mixtures whose constituents were chosen to represent the chemical families typically found asphalt binders. Asphalt binders have three main constituents i.e. asphaltenes, resins and maltenes. Asphaltenes are the most viscous and polar components; maltenes are mainly composed of aliphatic molecules and are least viscous and non-polar. Resins have properties that are in between of asphaltenes and maltenes. Greenfield and Zhang *(17)* chose n-docosane (n-C22H46) as a representative saturate for maltenes; 1, 7 dimethylnapthalene was chosen as representative Napthene aromatic i.e. representative element for resins and two different asphaltene structures were chosen based on the information available in the literature *(13)*. These asphaltene structures will be referred to as asphaltene-1 and asphaltene-2 and will also be used for molecular modeling in this research. To evaluate the effect of polymer modification on the

physical properties of asphalt binders, a single polystyrene chain of molecular weight 5223.6 g/mol was added to the asphaltene-2 based mixture.

Greenfield and Zhang *(17)* created two model asphalt mixtures using the following compositions of the three different representative molecules: 72% of n-docosane (saturates) 14% of 1, 7 dimethylnapthalene (resin) and 14 % asphaltene-1 or asphaltene-2. They reported the use of force field OPLS-aa (all atom optimized parameters for liquid simulations) for the simulations. They conducted molecular simulations at five different temperatures for both types of asphalt mixtures to analyze the properties with the variation in temperatures ranging from 230 K to 440 K i.e. very cold to extremely high pavement temperature conditions. Densities for each of the asphalt constituents were reported using molecular simulation methods. These densities were reported to be in good agreement with the literature values indicating the credibility of molecular simulation methods. Thermal expansion coefficient and bulk modulus values were also reported. SHRP core asphalts exhibit glass transition temperatures that range from -3.1 to -27.5 degree Celsius where as the values reported by Greenfield and Zhang using was above 25 degree Celsius. The short time scales accessible in molecular simulation might have lead to the discrepancies.

3. DETERMINATION OF INTRINSIC HEALING FUNCTION FOR ASPHALT BINDERS USING A DYNAMIC SHEAR RHEOMETER (DSR)

3.1 Introduction

Rheology is the study of the deformation and flow of matter under the influence of an applied stress such as a shear stress or tensile stress. The experimental characterization of a material's rheological behavior is known as Rheometry. Dynamic Shear Rheometer (DSR) is an experimental device that can be used to characterize the viscous and elastic behavior of asphalt binders. The DSR measures the viscous and elastic properties of a thin asphalt binder sample sandwiched between an oscillating and a fixed plate. When a force is applied to the sandwiched asphalt specimen, the DSR measures the response of the material, asphalt in this case, to the applied force. The relationship between the applied stress and the resulting strain in the DSR is used to quantify the complex shear modulus (G*) and phase angle (δ). G* is the ratio of maximum shear stress to maximum shear strain where as the phase angle is the time lag between the applied stress and the resulting strain.

3.2 Objective and Basic Approach

The primary objective of this task was to determine the relationship between the strength gained between two wetted surfaces of an asphalt binder as a percentage of the strength of the virgin binder with respect to time. In this research, the strength gained over time was quantified using the shear modulus measured using a DSR. The reasons for using shear modulus as a measure of strength are as follows: i) it can easily be measured using

the DSR which is a standard equipment in asphalt laboratory, and ii) it can be measured by applying very small stress or strain to the specimen and thereby not interrupting the healing process that may be occurring at the crack interface. Also, to develop this test procedure two circular asphalt specimens (of the same material) were brought into intimate contact with each other in order to obtain a completely wetted crack surface. This will be referred to as the two piece specimen in the remainder of this document. The increase in shear modulus of this two piece specimen was monitored over time using the DSR. In order to obtain properties of the virgin binder, a single specimen with a geometry equivalent to the two piece specimen was used. Section 3.4 and section 3.5 provides further details of this experiment and interpretation of the results.

3.3 Background on the Healing Mechanism Relevant to the Test Method

A precursor to the growth of a crack in a viscoelastic medium is the development of a fracture process zone at the crack tip *(18).* The fracture process zone can be considered to be comprised of a number of micro or nano cracks. An important distinction between the crack and the fracture process zone is as follows. A crack cannot support an external tensile load (considering Mode I failure); whereas, the capacity of the fracture process zone to support external tensile load varies from the end of the crack (zero ability) to that of the intact material. A common example of a fracture process zone is the formation of craze fibrils in thermoplastic polymers. Craze fibrils form following loss of entanglement of the molecular chains. At low temperatures and high strain rates, crazing occurs primarily due to scission of molecular chains, whereas at higher temperatures it occurs primarily due to disentanglement of molecular chains *(19).* One might argue that

the entanglement of long chains is not likely in asphalt, but work by Kim et al., *(20)* demonstrated the importance of asphalt functional group morphology and size on the healing process. Crack healing occurs immediately after removal of the external load. Figure 1 illustrates the crack tip with the zone of interest where the healing process is concentrated. The terminology used to describe the geometry and stresses in the healing process zone are borrowed from Schapery *(21)*. The length of the crack or healing process zone over which the intermolecular forces across the crack surfaces are effective in causing healing is denoted by $\boldsymbol{\beta}$. The tensile stress between the crack surfaces in the healing process zone is denoted by $\boldsymbol{\sigma}_b$. The rate at which the tip advances in the healing process zone to cause wetting between the crack surfaces is denoted by $\dot{a}_b$.

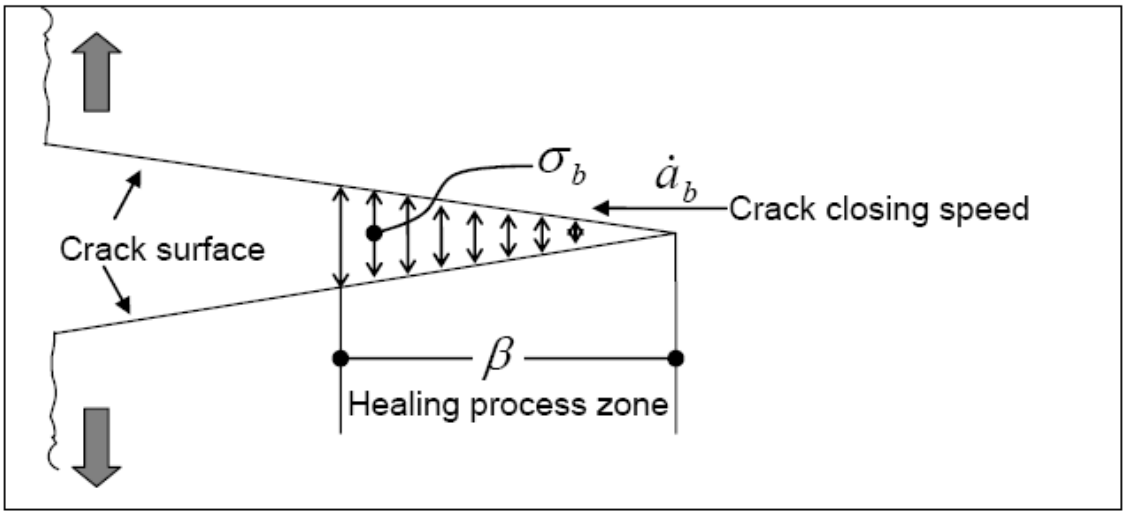

Figure 1: Crack Propagation and Fracture Process / Healing Zone in Mode I Loading

Based on the extensive work done in polymer healing by Wool and O'Connor *(1)* three primary stages of the healing process can be identified:

- wetting of the two faces of a nano crack,
- instantaneous strength gain due to interfacial cohesion between the crack faces, and
- long term strength gain due to diffusion and randomization of molecules from one face to the other.

de Gennes *(22)* proposed the reptation model to explain the movement of a polymer molecule in a worm like fashion inside a cross linked polymeric gel. Berger and Kramer *(19)* demonstrated that the disentanglement time for chains in the crazing zone during the crack growth process was in agreement with the reptation model. Wool and O'Connor *(1)* used the same reptation model but reversed the approach to determine the time required for healing caused by the inter diffusion of molecules between crack faces. They also realized that the overall rate of strength gain of a fractured interface due to healing is the net effect of the wetting and strength gain processes related to cohesion and inter diffusion. Based on this finding they ingeniously described net macroscopic recovery or healing in a material by combining an intrinsic healing function of the material with a wetting distribution function using a convolution integral as follows:

$$R = \int_{\tau=-\alpha}^{\tau=t} R_h(t-\tau)\frac{d\phi(\tau)}{d\tau}d\tau \qquad (2)$$

In Equation 2, *R* is the net macroscopic healing function, *R* (*t*) *h* is the intrinsic healing function of the material, φ (*t*, *X*) is the wetting function, and τ is the time variable. Succinctly stated, the convolution integral implies that the rate at which a crack regains

its ability to carry load or heal is the net effect of: i) the rate at which the two cracked surfaces wet and ii) the rate at which a wetted crack surface regains strength due to cohesion and inter diffusion. Lytton et al. *(23)* determined cumulative macroscopic healing as a function of time using a form very similar to the Ramberg-Osgood relationship. This is an excellent example of the macroscopic healing function *R* over time, which is the result of the two processes described above. A more detailed description of the two functions that describe the two processes related to healing follows. The wetting distribution function, φ (*t*, *X)*, defines wetting at the contact of the two crack surfaces in a domain *X* over time *t.* Fundamental properties such as the surface free energy, viscoelastic properties, and fracture toughness of the bitumen dictate the rate at which the two crack surfaces wet each other. For example, bitumen with higher surface free energy will have stronger intermolecular forces of attraction between the two cracked surfaces and will consequently wet at a faster rate. The analytical form for the wetting function can be simplified by considering wetting that occurs at a constant rate, or for instantaneous wetting. The wetting function reduces to a constant for the former case and to a Dirac-delta function for the latter. The domain in which wetting occurs is dictated by the geometric considerations for crack growth within the material. The following sub-section presents an analytical form for the healing function. This analytical form relates the wetting function or rate of wetting to the material properties of the bitumen. The intrinsic healing function, R_h (*t*) , defines the rate at which two crack faces that are in complete contact with each other (are wetted) regain strength due to the interfacial work of cohesion between the crack faces and inter diffusion and

randomization of the molecules from one face to the other. Material properties such as the surface free energy and coefficient of self diffusion dictate the magnitude and rate at which a wetted crack interface regains strength. For example, bitumen with higher surface free energy and hence higher work of cohesion will have higher instantaneous strength gain. Also, bitumen with a higher coefficient of self diffusion will facilitate faster inter diffusion of molecules and promote the rate of strength gain.

3.3.1 Wetting Function

The first step in the healing process, i.e., wetting of the two faces of a nano crack is represented by a wetting distribution function φ (*t*, *X)* as described in the convolution integral (equation 2). This section presents an explicit relationship between the wetting distribution function and material properties related to the wetting for a one dimensional case. Schapery *(21)* developed a relationship between the work of cohesion and the material properties related to the wetting of crack surfaces. Based on this relationship, the wetting distribution function or rate of wetting of a crack surface can be shown as follows:

$$\frac{d\phi(t,X)}{dt} = \dot{a}_b = \beta\left[\frac{1}{D_1 k_m}\left\{\frac{\pi Wc}{4(1-\nu^2)\sigma_b^2\beta} - D_0\right\}\right]^{-\frac{1}{m}} \quad (3)$$

In Equation 3, *Wc* is the work of cohesion; ν is the Poisson's ratio; D_0, D_1, and m are creep compliance parameters obtained by fitting $D(t) = D_0 + D_1 t^m$; and k_m is a material constant that can be computed from m. The terms σ_b, β , and $\dot{a}_b$ are as described before (Figure 1). The wetting function described in Equation 3 represents a case of wetting that occurs at a constant rate. The value of the constant rate at which

wetting occurs is determined by mechanical, viscoelastic and material properties of the bitumen.

The dimensional consistency of Equation 2 can easily be verified. The right hand side of Equation 3 contains mechanical and viscoelastic properties of the material, i.e., Poisson's ratio and creep compliance parameters. These properties can be easily determined using laboratory tests. The right hand side of equation 3 also contains three material properties, i.e, the work of cohesion (W_c), the length of the healing process zone (β), and the tensile stresses that cause the crack faces to close (σ_b). In most cases healing is quantified in terms of the percentage of strength gained before and after the rest period. To represent such a case, the wetting distribution function must be modified in order to represent the fraction of the newly formed crack surface that wets during the healing process. For a one dimensional case, this can be done by eliminating the domain *X* and normalizing the crack growth function in equation 3 with the length of the crack that has grown in N cycles, ΔR_N , as follows:

$$\frac{d\phi(t)}{dt} = \frac{\beta}{\Delta R_N}\left[\frac{1}{D_1 k_m}\left\{\frac{\pi W c}{4(1-v^2)\sigma_b^2 \beta} - D_0\right\}\right]^{-\frac{1}{m}} \quad (4)$$

where,

β ' = β , when β < ΔR_N

= ΔR_N, when β ≥ ΔR_N .

The substitution for β in Equation 3 to obtain Equation 4 provides a form that is consistent with the observed healing behavior in asphalt mixtures. Consider a case when rest periods are provided very frequently such that the incremental crack growth is small

and the incremental length of the crack does not exceed the length of the healing process zone ($\beta \geq \Delta R_N$). For example, Carpenter and Shen *(4)* evaluate the effect of healing on endurance limit by providing a rest period after every load cycle. A similar effect can also be obtained by adding fine well dispersed filler in the asphalt mastic. For example, Kim et al. *(3)* demonstrate the effect of introducing hydrated lime filler particles on the healing of asphalt mastics. In such a case the wetted length is maximized simply because the incremental crack progression is kept within a certain critical limit and the entire crack can heal (although it might not gain the same strength as the original binder). This is discussed in the following sub section on the intrinsic healing function, $R_h(t)$. On the other hand, if rest periods are spaced apart so that significant crack growth occurs before a rest period is provided, i.e., $\beta < \Delta R_N$, then the maximum healing length of the crack is limited to the length of the healing process zone. The tensile stresses that cause the crack faces to close (σ_b) can be considered to be directly proportional to the surface free energy or the work of cohesion of the material (W_c). This is a reasonable assumption since materials with higher surface free energy would also have a higher affinity to cohere and develop greater tensile stresses between the two surfaces. Based on the typical order of magnitudes of the various parameters, the contribution of the creep compliance parameter, D_0 , can be neglected. Based on this consideration, it is easy to see from equation 3 that materials with significantly higher work of cohesion will have a higher rate of wetting and consequently healing.

3.3.2 Intrinsic Healing Function

The second and third steps of the healing process, i.e., strength gain due to interfacial cohesion and inter diffusion of molecules between the wetted surfaces is represented by the intrinsic healing function $R_h(t)$ as described in the convolution integral (Equation 2). This section presents a functional form for the intrinsic healing function along with a brief discussion on the significance of the parameters used in the functional form. Section 4 of this paper presents a new and simple test method to obtain the parameters for the intrinsic healing function. Based on Einstein's relation for a 'one dimensional random walk in the tube', Wool and O' Conner *(1)* demonstrated that the intrinsic healing function is best represented using the following form:

$$R_h(t) = R_0 + Kt^{0.25} \bullet \varphi(t) \qquad (5)$$

In Equation 5, t is the time, and ϕ (t) is used to represent the effect of time surface rearrangement of molecules. The symbol • represents the convolution process. This model was developed for simple polymer molecules and for short time healing. Wool and O' Conner also report that for longer duration the power factor changes from 0.25 to 0.5. The healing function represents the sum effect of: i) instantaneous strength gain due to interfacial cohesion at the crack interface, represented by the parameter R_0 , and ii) time dependent strength gain due to inter diffusion of molecules between the crack surfaces, represented by $Kt^{0.25} \bullet \phi$ (t). In this study, a sigmoid function was used to represent the latter. The sigmoid function for time dependent strength gain or healing is similar to the form that is used to model other processes such as kinetics of phase

transformations in solids *(24)*. The form of the healing function that was used is shown below (Equation 6).

$$R_h(t) = R_0 + p\left(1 - e^{-qt^r}\right) \quad (6)$$

$R_h(t)$ is a time dependent dimensionless function that represents the increase in a mechanical property of the wetted crack interface, typically as a fraction or percentage of the same property for the intact material. This function can be used to represent any mechanical property of interest, for example, shear modulus. Since R_0 reflects the effect of instantaneous healing due to cohesion at the crack interface, its magnitude is expected to be proportional to the work of cohesion or surface free energy of the material. Section 3.5 demonstrates the validity of this hypothesis. Since this parameter depends on the surface free energy of the material, it would also depend on extrinsic properties such as temperature. The parameters, p, q, and r, represent the effect of healing that is due to the inter diffusion of molecules between the crack surfaces. Therefore, these parameters will be dictated by intrinsic material properties such as molecular weight, and activation energy for diffusion. In addition, these parameters will also depend on extrinsic properties such as pressure and temperature. By testing different materials under similar conditions the effect of extrinsic properties on the healing function parameters can be eliminated. In this test method, 25 degree Celsius temperature and an approximate normal force value of 0.4 Newton is maintained for all the tests to determine the complex shear modulus values. This complex shear modulus values are used to determine $R_h(t)$ functions for three different types of binders, AAM, ABD and AAD.

The $R_h(t)$ values in turn are used to calculate the four parameters of the healing characteristic equation (Equation 6); R_0, p, q and r.

Two separate thin circular asphalt binder specimens are used to simulate the two surfaces. Here, the important point to be noticed is that these two surfaces are not the ones generated from cracking. Solidified asphalt which is stored at temperatures close to 45 degree Fahrenheit is taken and heated in the oven at temperatures close to 100 degree Celsius. This heated liquid asphalt is solidified back at room temperature while preparing the test specimens. This solidification is a slow process and results into smooth surfaces which means literally there are no end chains for the immediate diffusion. Thus, the diffusion initiation function, $\Omega(t)$, has a big role to play in the healing process of these samples.

3.4 Test Procedure Using DSR to Determine the Intrinsic Healing Function

The following test procedure was used to determine the intrinsic healing function for different asphalt binders:

1. Asphalt binder stored at 45 degree Fahrenheit was taken and placed in an oven at temperature close to 100 degree Celsius for 30 minutes.

2. The heated asphalt which was in the liquid state was taken and poured in the molds to prepare test specimens. The liquid asphalt in the mold was allowed to solidify at room temperatures for 30 minutes.

3. After allowing the samples to settle in the mould for 30 minutes, the thicknesses and weights of the samples were measured. The specimens were circular shaped

with radius of18 mm. The average thickness of the samples was around 3.5 mm and the average weight is around one gram. It was ensured that the dimensions of all the specimens tested in this project were consistent. `

4. Advanced Rheometer (AR), AR 2000, was used to test the specimens. AR maintains constant normal force during the test which is a feature normally not available with conventional DSRs. The AR maintains the required normal force by changing the gap accordingly during the experiment. Adjustment of gap is a slow process and hence it should be expected that there will be some difference between the required normal force and the normal force applied during the experiment. In the experiments for this project a normal force of 0.4 N is used. The error margin of the equipment used is 0.1 N and hence the normal force values during the experiment varied from 0.3 to 0.5 N. The AR allows the user to have a precise control of the stress or strain that is applied to determine the shear modulus. A constant strain of 0.001% was applied to determine the shear modulus in all experiments for this research. An extremely small strain was selected so that the disruption of the asphalt interface undergoing healing would be minimal. Low strains of this order may not possible with a conventional DSR. It should also be noted that the complex shear modulus values are highly sensitive to the applied shear strains and thus the equipment such as AR with better control over the strains, yields better results.

Another advantage of AR is its ability to maintain the temperature. With a conventional DSR, the test specimen is immersed in the water bath in order to control its temperature. This is not desirable for healing experiments since the presence of water can effect the rate of healing. In this project all the tests were done at room temperature i.e. at 25 degree Celsius.

Before starting the test the Rheometer was prepared in the following manner:

- The base plate and parallel plate spindle were attached to the Rheometer. After attaching these test fixtures, Rheometer panel shows the readings of pressure, temperature and strains. Adjustments should be made for pressure if required. Pressure should not go less than 30 MPa.

- Mapping was performed so that the software is intimated of the changes in test fixtures and for appropriate required calibration.

- Gap between the spindle and base plate was zeroed by bringing the spindle into contact with the base plate. This means that the software measures the gaps with respect to the base. Spindle was raised back after zeroing.

- Following was the input data used for testing: Temperature = 25 degree Celsius, Strain = 0.001%, Normal Force = 0.4 N, Allowed variation in normal force = 0.1 N, Allowed variation in the gap while

maintain the normal force = 10,000 micron. 'Control normal force' option was activated.

5. Details of the test procedure used for the experiments in this research were as follows: the complex shear moduli (G*) was measured at the end of 0, 2, 4, 6, 8, 10, 15, 20, 25, 30, 40, 50 and 60 minutes. A constant normal force of 0.4 N is maintained. The complex shear moduli was measured by applying a cyclic load with a strain amplitude of 0.001 % and at 10 rad/sec frequency. The readings were taken for a time span of 5 seconds after each of the above mentioned time intervals. One point worth noting here is that the equipment continually measures complex shear moduli during that span of five seconds while trying to achieve the target strain. However, only the moduli of measured at a strain rate closest to 0.001% were used for further analysis.

6. One of the asphalt specimens was attached to the spindle and the other specimen to the base at a point exactly below the spindle so that the center lines perpendicular to the circular planes of the two specimens coincides, Figure 1 (a). Normal force was zeroed at this point so that the self weight of the upper specimen is not considered while calculating the normal forces.

7. The spindle was lowered up to the point where the gap between the spindle and the base is 5000 micron, Figure 1 (b). Here it should be noted that the average thickness of the test specimen is 3500 micron. Thus the combined thickness of the two test specimens is around 7000 micron. Thus, the binder is compressed up

to 2000 micron. It should be taken care that this compression process is completed within one minute after the specimens come into contact. Therefore, the test starts at the end of this one minute i.e. one minute after the specimens come into contact i.e. one minute after the start of actual healing process.

Ideally, it is required to make measurements immediately after the specimens come into contact. However it is difficult to determine the exact time at which the specimen surfaces come into complete contact with each other. Thus, to simplify this stage of healing process, within a minute, the surfaces of the two test specimens are brought into intimate contact with each other due to the applied load. The processes within this one minute time window were neglected and the measured property at this time was treated as the property at time t=0 or instantaneous property.

This also justifies the assumption of instantaneous wetting. Thus, the wetting distribution function $\varphi(\tau, X)$ is assumed to be $\delta(\tau)$, Dirac-delta function. A similar assumption cannot be made with diffusion initiation function $\Omega(t)$. Though the surfaces are in contact, it is not necessary that the diffusion process at all the points of the surface is completed within that one minute.

8. Test was started as soon as reaching to a gap of 5000 micron. It may be difficult always to reach the exact point of 5000; +/- 10 micron was considered as acceptable. Also, when it was not always possible to reach the 5000 micron gap

exactly at the end of one minute after the contact; +/- 5 seconds was considered as acceptable. Test runs for an approximate hour and all the results will be saved automatically. After the test the spindle was brought back to its default position, Figure 1 (c). The effect of healing on the two binders can be seen from Figure 1 (c).

9. In the healing equation, R is defined as the dimensionless recovery ratio representing the extent of healing. It is the ratio of the property as it heals with that of the intact material. From the above explained test procedure we can find the complex shear modulus values of the combined specimen as they heal with time. To determine "R" we also need to find the "G*" value of intact binder specimen with respect to time. Ideally, there should be no change in the value of G* of the intact specimen with time. However, since a small normal load is continually applied some creep and concomitant change in G* can be expected. Other factors, such as steric hardening may also contribute to the change in G* over time for the intact specimen. The same testing procedure as before was used to determine the G* for a single intact specimen over time. A single specimen of thickness equals to twice of the original test specimens i.e. 7000 micron was used for this purpose so that the exact boundary conditions are replicated in both the cases.

10. Asphalt specimens should be cleaned from DSR plates as soon as possible after the completion of the test; sooner they are cleaned, easier to do that.

a) Two bitumen specimens affixed to the two end plates of the DSR

b) Bitumen specimen after being brought into contact with each other to measure change in composite G* over time

c) Separation of the test specimens after completion of the test

Figure 2: DSR Test Procedure

3.5 Results

Three asphalt binders (AAM, AAD, and ABD) were used in this research project. Selection of these asphalt binders was based on the availability of the data from literature which can be related to healing characteristics which in turn can be related to the results if the DSR test method. For example short term healing rate can be related to surface energy of asphalt binders. Subsection 3.4 describes the test method to obtain the increase in shear modulus with respect to time as the healing occurs across in the interface of a two piece specimen. The following procedure was used to compute R (t) from the DSR test results for the selected binders.

After the experiment the data was exported to Excel sheets. The data which was exported for healing analysis included G*, Gap, Normal Force, % strain and Time (Global). Once the data was transferred, the shear modulus values were carefully examined. There were typically three to five values of shear modulus that were recorded at each loading time span of 5 seconds. Out of all the output values at each point in time the shear modulus value at strain rate which is closest to 0.001 radian per second (the design strain rate) was considered for analysis. Figure 3 illustrates a typically variation in shear modulus with respect to time for a two piece specimen. Figure 4 illustrates a similar graph for the intact single piece specimen for AAM binder . As discussed before, the reason for increase in the shear modulus with time for the intact specimen could be due to the continually applied normal load (albeit small in magnitude) and changes in the micro structure of the binder itself. The healing percentage at any given time point is calculated as the ratio of shear modulus of the two piece binder specimen with that of the single piece binder specimen. Figure 5 shows the healing percentage for AAM with respect to time. The data of Figure 5 can also be used to determine the parameters of healing characteristic equation i.e. Equation 4. Solver function in Excel is used to determine the values of four parameters. The calculated values of the four parameters for AAM are as follows: R_0 = 55, p = 66, q = 7E-05 and r = 2.01.

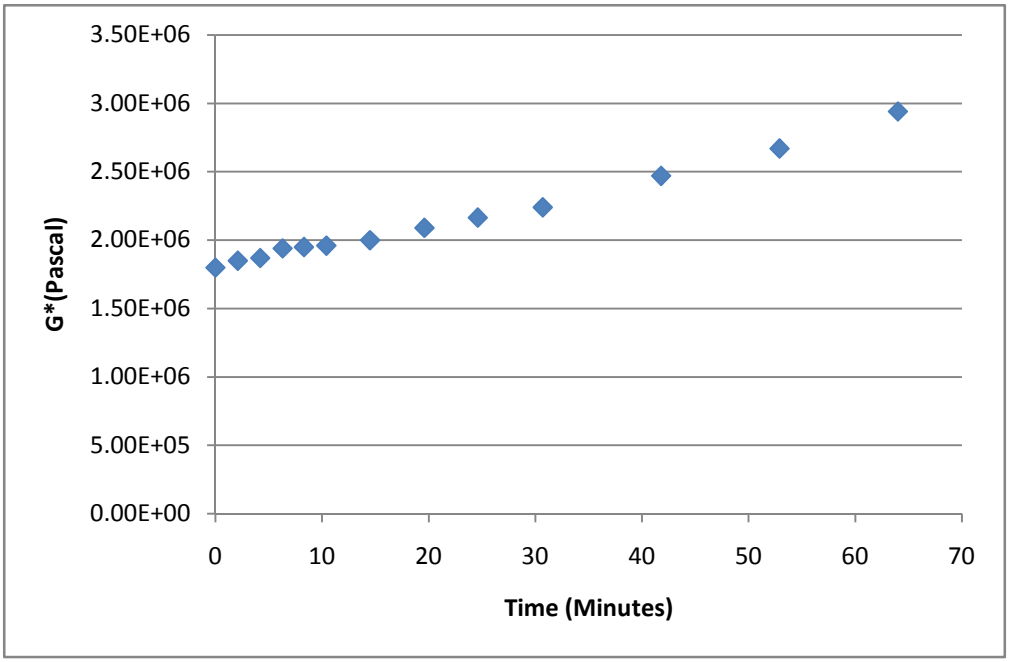

Figure 3: Change in Shear Modulus due to Healing (AAM)

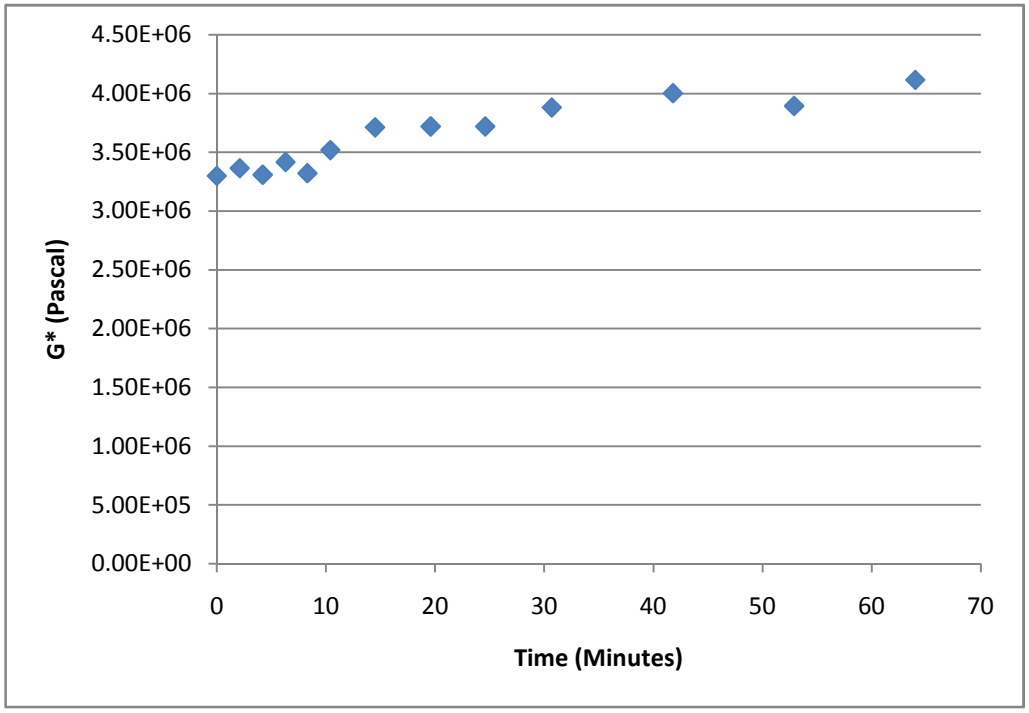

Figure 4: Change in Shear Modulus (Virgin Binder, AAM)

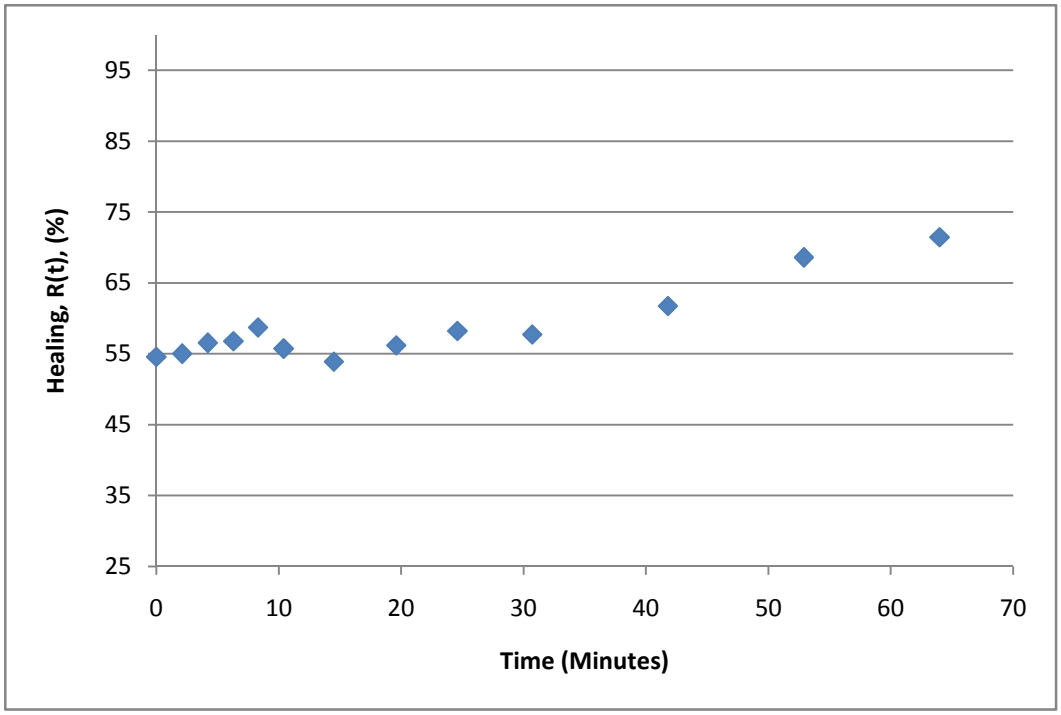

Figure 5A: Healing, R (t), (%), AAM

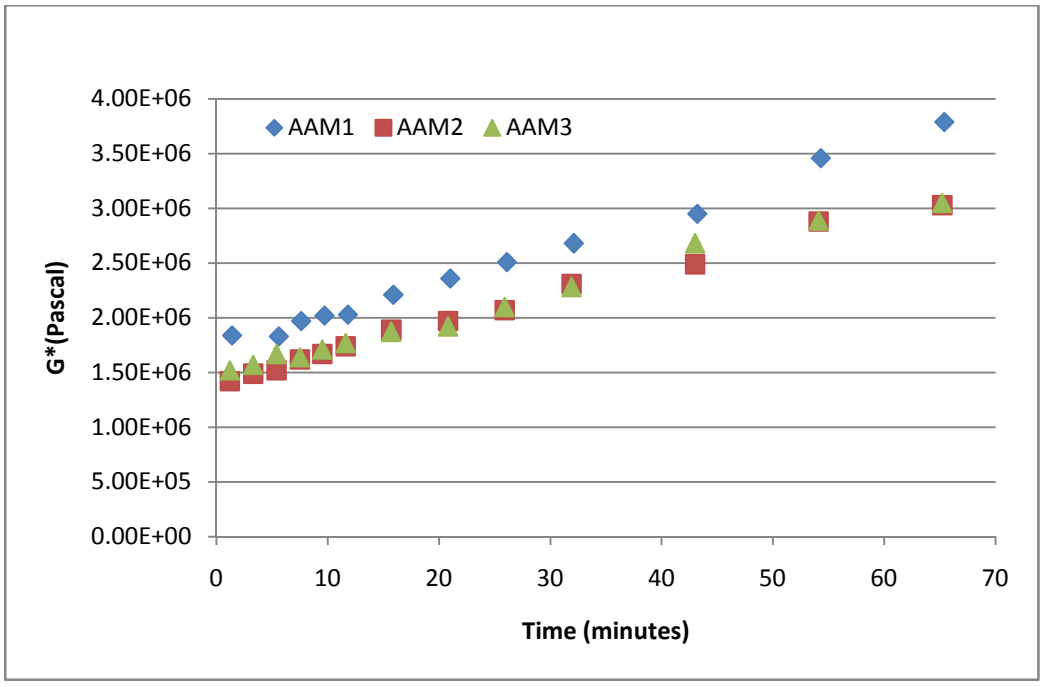

Figure 5B: Repeatability of the Test Results

Figure 5A shows the repeatibility of the test results. The results of the three tests conducted on AAM asphalt binders shows that the test method gives consistent experimental results. Similar testing and analysis is done on other two binders AAD and ABD. The results for AAD are shown in Figure 6, Figure 7 and Figure 8 where as the result for ABD are shown in Figure 9, Figure 10 and Figure 11.

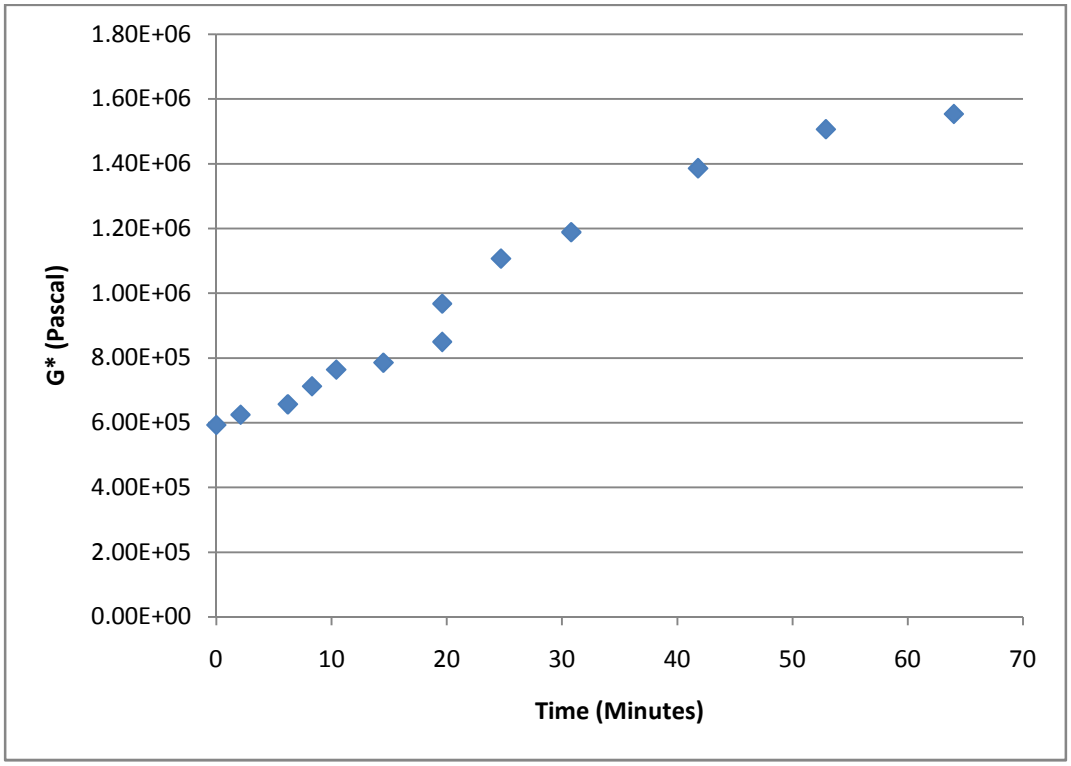

Figure 6: Change in Shear Modulus due to Healing (AAD)

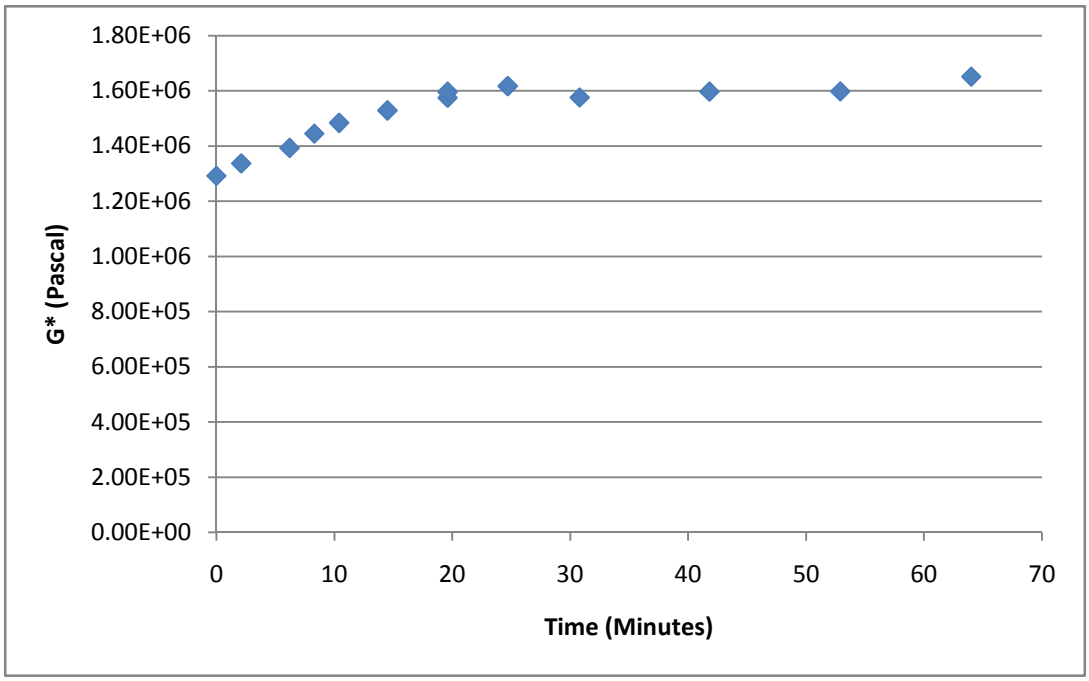

Figure 7: Change in Shear Modulus (Virgin Binder, AAD)

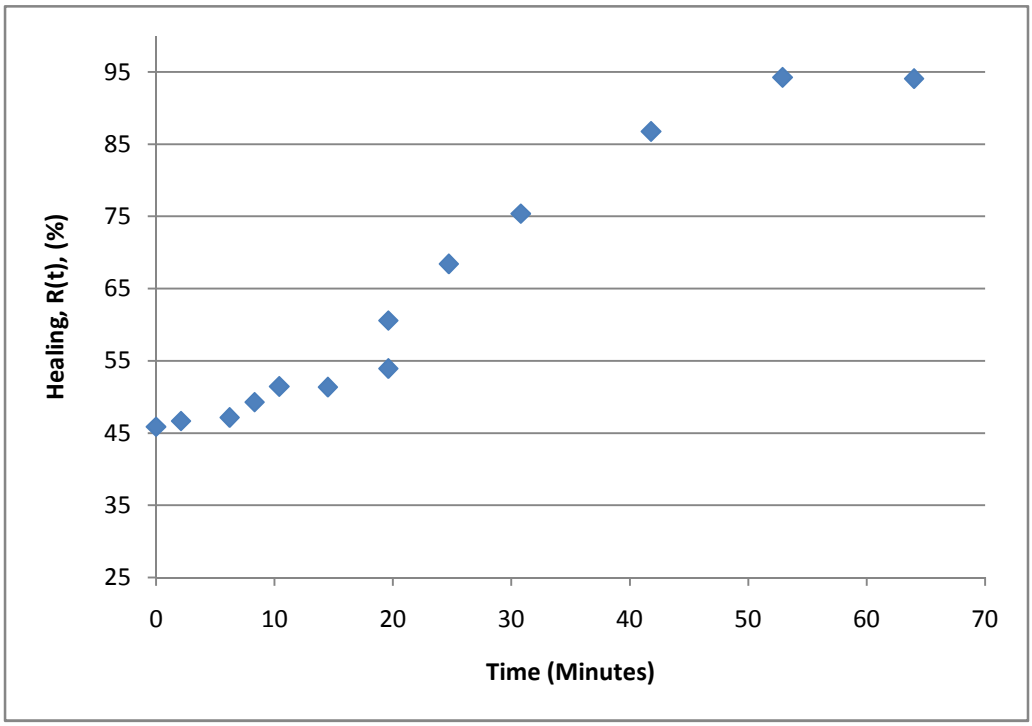

Figure 8: Healing, R (t), (%), AAD

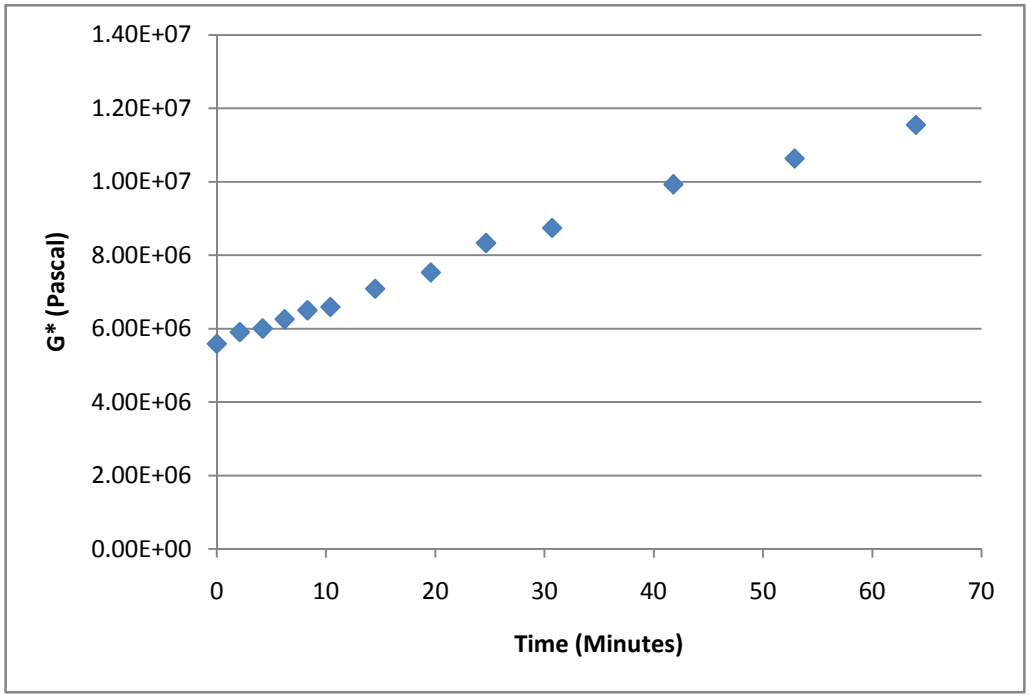

Figure 9: Change in Shear Modulus due to Healing (ABD)

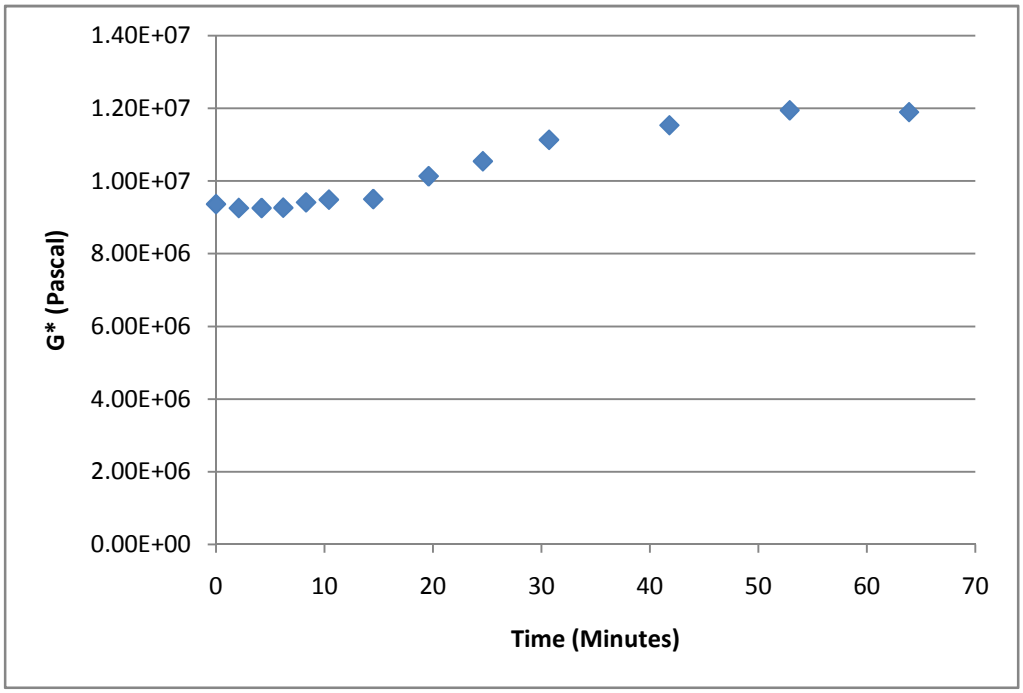

Figure 10: Change in Shear Modulus (Virgin Binder, ABD)

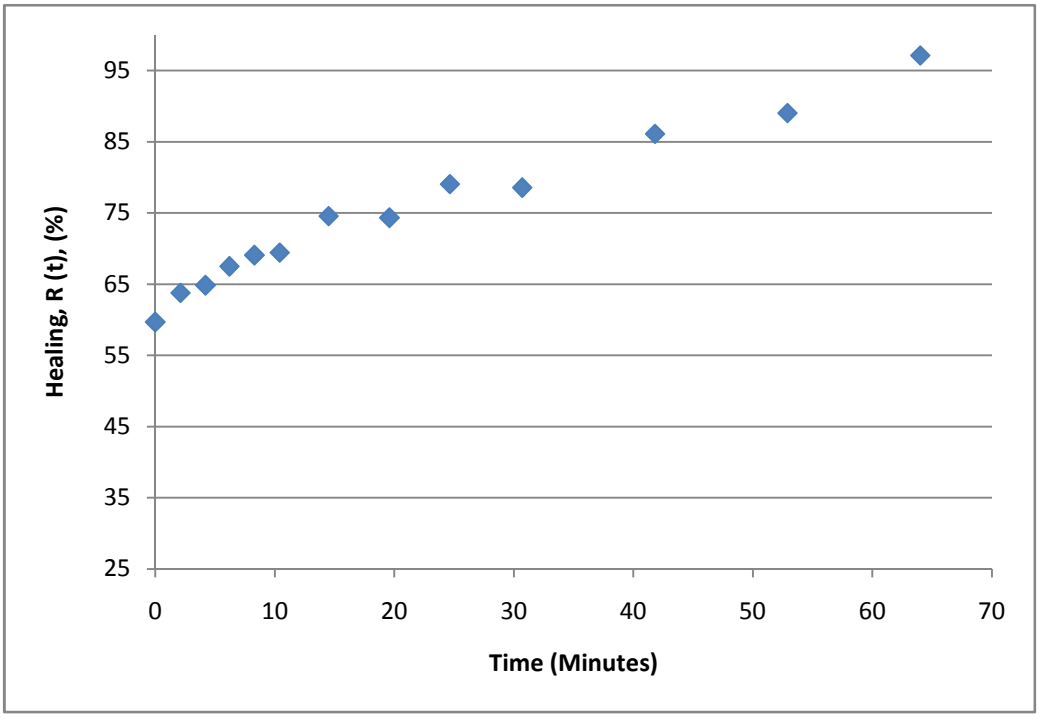

Figure 11: Healing, R(t), (%), ABD

The data which was used for making the figures was also used to determine the parameters of the healing characteristic equation, Equation 6. The calculated values of the parameters are as shown in the Table 1.

Table 1: Parameters for the Healing Function

Bitumen	R_0	p	q	r
AAD	39	60	2.E-03	1.73
AAM	55	66	7.E-05	2.01
ABD	60	1728	1.E-03	0.69

3.6 Discussion

Figure 12 illustrates the different healing patterns that are followed by the three different binders. The data showed in this figure is the average of the three replicates for each of the three binders. From the figure it can be observed that AAM has high short term healing rate compared to AAD where as the trend reverses in case of long term healing. Among the three binders, ABD has highest both short term and long term healing rates. It can also be observed from the figure that AAD has the highest increase in R (t) compared to the other two binders.'R_o' represents the instantaneous healing nature of the binders and hence the effect of this parameter on the characteristic equation is analogous to the effect of surface energy on actual healing. Figure (13) shows the comparison of the trends of 'R_o' values with that of surface energy values. As expected the values of 'R_o' are directly proportional to the values of surface energy. These surface energy values which are taken from the literature are the values calculated using Wilhelmy Plate method.

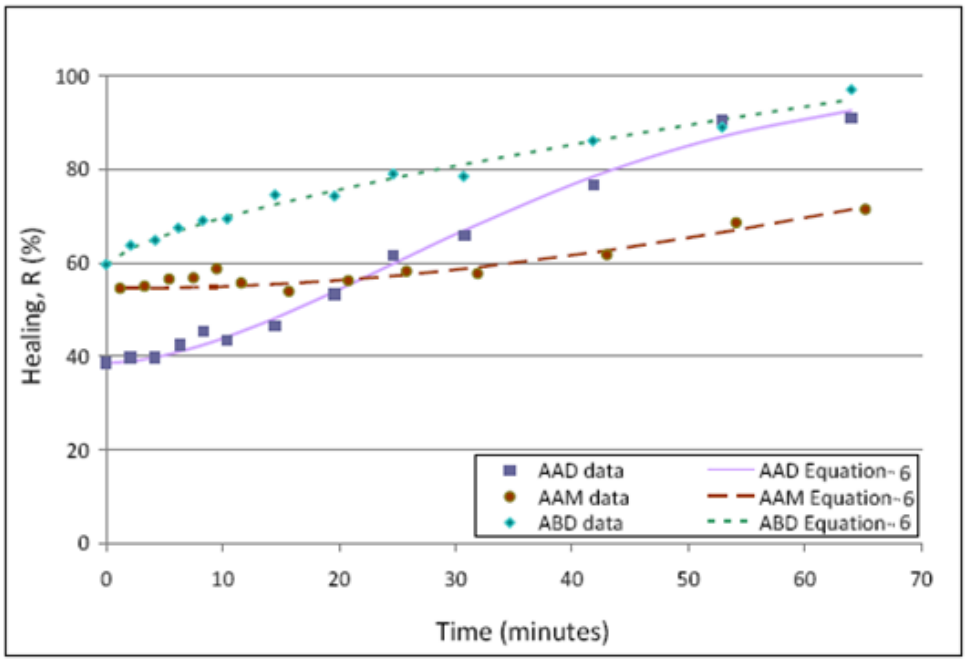

Figure 12: Healing Function, for Selected Bitumen, Obtained Using the DSR Data

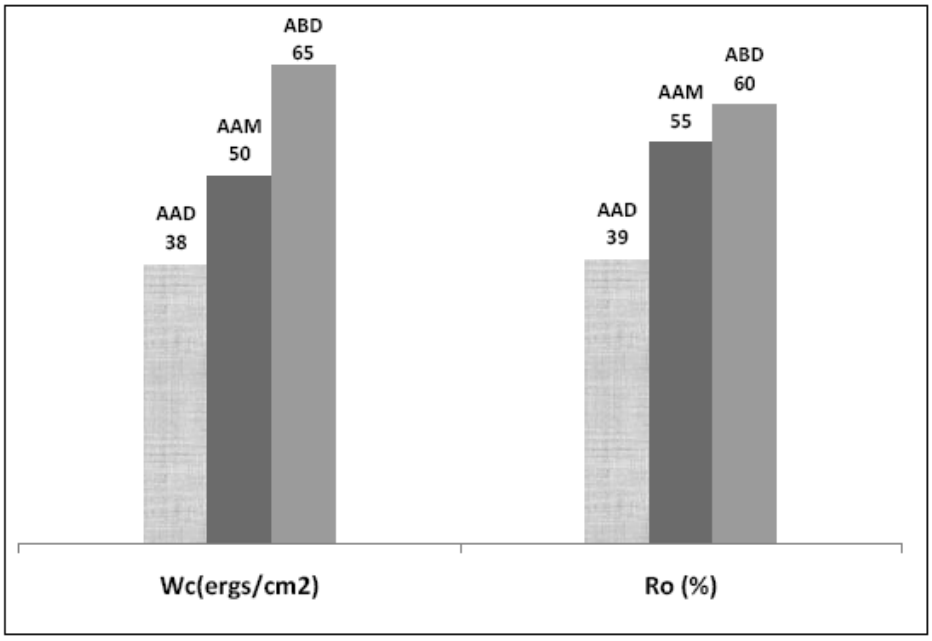

Figure 13: Surface Free Energy vs. Parameter of Instantaneous Healing (Ro) from DSR Data

4. MOLECULAR MODELING METHOD

4.1 Introduction

In this research, molecular modeling analysis was used to determine the influence of morphology of asphalt molecules on its healing characteristics. Two properties that are related to healing in asphalt binders are its surface free energy and diffusivity. Molecular modeling techniques were used to determine the influence of molecular morphology on the surface free energy and molecular diffusion coefficients for various types of asphalt binders.

"Materials Studio" software was used for molecular modeling. In order to conduct molecular simulations it is required to represent the asphalt binders by their molecular structures. Since the chemical makeup of asphalt binders is very complicated it is extremely challenging to develop an exact representative ensemble of molecules for different types of asphalt binders for simulation. Determination of chemical structure of asphalt binders in itself is an active research area. In this research the following two different approaches were used to represent the molecular structure and composition of asphalt binders : 1) Average molecular structure representing the different asphalt binders and determined using NMR spectra were adopted from the SHRP-A-335 report (Appendix-1 details all the eight SHRP structures used in this project) and 2) in the second approach, a hypothetical asphalt binder was created by considering its three constituents i.e. asphaltenes, napthene aromatics and saturates. A unique molecular structure representing each of these three constituents was adopted from the literature *(17)*.

One of the objectives of this task was to determine the influence of morphology of molecules on the healing characteristics of asphalt binders. Surface free energy and molecular diffusion play a predominant role in asphalt healing. Surface energy can be well related to the healing at initial stages i.e. short term healing, where as diffusion characteristics affects the long term healing of asphalt. The following sections described the protocols that were developed using Materials Studio to determine the surface free energy and molecular diffusion coefficients.

4.2 Background on Energy Minimization and Molecular Dynamics Used During Simulations

The two main process in molecular modeling analysis are energy minimization and molecular dynamics.

4.2.1 Energy Minimization

Energy Minimization or optimization (with respect to potential energy) is the first and most important step in any molecular simulation. A conventional two dimensional representations or sketch of a complex molecular often represents a high energy configuration. It is therefore desirable to optimize/minimize a molecular structure after it has been created. The minimization process adjusts the geometry and conformation of the molecule so that it is in a low energy state. The optimization of a structure is a two step process: energy evaluation and confirmation adjustment.

4.2.1.1. Energy Evaluation

First an energy expression must be defined and evaluated for a given conformation. Energy expression is the equation that describes the potential energy surface of a particular molecular structure as a function of its atomic coordinates. The coordinates of a structure combined with a force-field create an *energy expression*. The potential energy of a system can be expressed as a sum of valence (or bond), cross term, and non-bond interactions:

$$E_{total}=E_{valence} + E_{cross\ term} + E_{non\text{-}bond} \quad (7)$$

Equation 8 is an example of the corresponding general, summed force field function:

$$\begin{aligned} V(R) = & \sum_b D_b\left[1-\exp\left(-\alpha\left(b-b_0\right)\right)\right]^2 + \sum_\theta H_\theta\left(\theta-\theta_0\right)^2 + \sum_\phi H_\phi\left[1+s\cos\left(n\phi\right)\right] \\ & + \sum_\chi H_\chi\,\chi^2 + \sum_b\sum_{b'} F_{bb'}\left(b-b_0\right)\left(b'-b_0'\right) + \sum_\theta\sum_{\theta} F_{\theta\theta'}\left(\theta-\theta'\right)\left(\theta-\theta_0'\right) \\ & + \sum_b\sum_\theta F_{b\theta}\left(b-b_0\right)\left(\theta-\theta_0\right) + \sum_\theta\sum_\theta F_{\theta\theta'\phi}\left(\theta-\theta'\right)\left(\theta-\theta_0'\right)\cos\phi \\ & + \sum_\chi\sum_{\chi'} F_{\chi\chi'}\,\chi\chi' + \sum_i\sum_{j>i}\left[\frac{A_{ij}}{r_{ik}^{12}} - \frac{B_{ij}}{r_{ij}^{6}} - \frac{q_i q_j}{r_{ij}}\right] \end{aligned} \quad (8)$$

The first four terms in this equation are sums that reflect the energy needed to:

- stretch bonds (b)
- bend angles (θ) away from their reference values
- rotate torsion angles (ϕ) by twisting atoms about the bond axis that determines the torsion angle
- distort planar atoms out of the plane formed by the atoms they are bonded to (χ)

The next five terms are cross terms that account for interactions between the four types of internal coordinates. The final term represents the non-bond interactions as a sum of repulsive and attractive Lennard-Jones potential terms as well as Columbic terms, all of which are a function of the distance (r_{ij}) between atom pairs. In this expression force field define the bond lengths (b) and angles (θ), the functional form and the force constants (K). The force field describes approximately the potential energy hyper surface on which the atomic nuclei move. Force fields are usually tuned for particular groups of systems, so the choice of force field will depend on the type of structure that is being investigated. The force field used in this research is Compass. The reason for using Compass (Condensed-phase Optimized Molecular Potentials for Atomistic Simulation Studies) force field is, it is the first ab-initio force field that enables accurate and simultaneous prediction of gas-phase properties (structural, conformational, vibrational, etc.) and condensed-phase properties (equation of state, cohesive energies, etc.) for a broad range of molecules in polymers. It is also the first high quality force field to consolidate parameters of organic and inorganic materials.

The energy expression in Equation 8 is cast in a general form. The true energy expression for a specific structure includes information about the coordinates that are included in each sum. For example, it is common to exclude interactions between bonded and 1-3 atoms in the summation representing the non-bond interactions. Thus, a true energy expression might actually use a list of allowed interactions rather than the full summation implied in Equation 8.

4.2.1.2 Conformation Adjustment

Once the energy expression for the initial confirmation is fixed, the conformation is adjusted to minimize the energy. A minimum may be found after one adjustment or may require many thousands of iterations, depending on the nature of the algorithm, the form of the energy expression, and the size of the structure. The efficiency of the optimization is therefore judged by both the time needed to evaluate the energy expression and the number of structural adjustments (iterations) needed to converge to the minimum. In this research work, following parameters are used for energy minimization:

- Minimization method = Conjugate Gradient method
- Convergence level of 0.1 k Cal/Mole/ A^0
- Non bond cut off energy limit for Vander Waals forces = 8.5 A^0
- Spline width and buffer width are 1 A^0 and 0.5 A^0 respectively
- Maximum number of iterations = 2000 and
- Atom based summation method for van der Walls forces and Cell Multi-Pole based summation method for coulomb forces.

Conjugate gradient method is the general choice for the minimization of large models. Time per iteration may be longer for conjugate gradients than for other general minimization methods like steepest descents, but this time factor is more than compensated for by the more efficient convergence to the minimum achieved by conjugate gradients. Convergence level is the level of accuracy used for assessing the convergence of the specified minimization method. Non-bond cut off energy limit for van der Walls force is the cut-off distance for the calculation of non-bond interaction

energy; the interactions beyond the cut-off distance are simply ignored. Spline width is the region within which non-bond interactions are to be splined from their full value to zero when the cubic spline truncation method is used. A spline width of zero switches off spline interpolation and is equivalent to a direct cutoff. Buffer width is to be used when creating the non-bond neighbor lists. When any interaction pair moves more than half this distance, the neighbor list (if used) is recreated. This does not affect any values calculated, but do affect the computation time.

4.2.2 Molecular Dynamics

After setting the energy expression and after adjusting for an optimized conformation, a dynamics simulation can be run. The basis of this simulation is the classical equations of motion which are modified, where appropriate, to deal with the effects of temperature and pressure on the system. The main product of a dynamics run is a trajectory file that records the atomic configuration, atomic velocities and other information at a sequence of time steps which can be analyzed subsequently.

The typical parameters used for molecular dynamics process are as follows:

- Force Field = Compass
- Ensemble = NVT
- Temperature = 298 K
- Equilibrium duration = 0.5 ps
- Dynamics duration = 5 ps
- Time step for each cycle = 1 fs.

NVT indicates that the molecular dynamics were conducted at constant volume and constant temperature. The dynamics are modified to allow the system to exchange heat with the environment at a controlled temperature. A temperature of 298 K was chosen since the objective was to determine and compare properties of the asphalt binder at room temperature. Dynamics duration was chosen to be 5 pico seconds. Longer duration of dynamics are desirable but 5 ps was selected keeping in view the available computer resources and time constraints. Time step for each cycle was chosen as one femto second and a frame is extracted after each 100 femto seconds. Thus fifty frames are extracted within the duration of dynamics i.e. 5 pico seconds. Diffusion characteristics were calculated by selecting a frame with a conformation that had the least energy from the trajectory of these 50 frames. Using these minimization and dynamics parameters, analysis protocols were developed to determine the surface free energy and molecular diffusion coefficients. The step by step protocols developed and used to obtain each one of these parameters are explained in next section, Section 4.3.

4.3 Testing Procedure

Procedure to determine surface free energy and molecular diffusion coefficients are explained in this section. This detailed procedure is demonstrated using a hypothetical asphalt binder comprising of 20% asphaltenes (by weight), 40% napthene aromatics and 40% of saturates is chosen.

4.3.1 Method to Determine Surface Energy

The step-wise procedure to determine the surface energy is as follows:

I. Sketching of Molecules:

Molecules which are to be used in the molecular modeling analysis were sketched using the Sketch function in Materials Studio software or imported from other existing files, when available. The sketches of the three constituents are as shown in Figure 14. The details of the molecules are as follows:

- Asphaltenes: Asphaltenes are mixed paraffin-napthene aromatics in polycyclic structures with traces of sulfur, oxygen and nitrogen. The structure of the asphalt is as shown in Figure 14 (a).

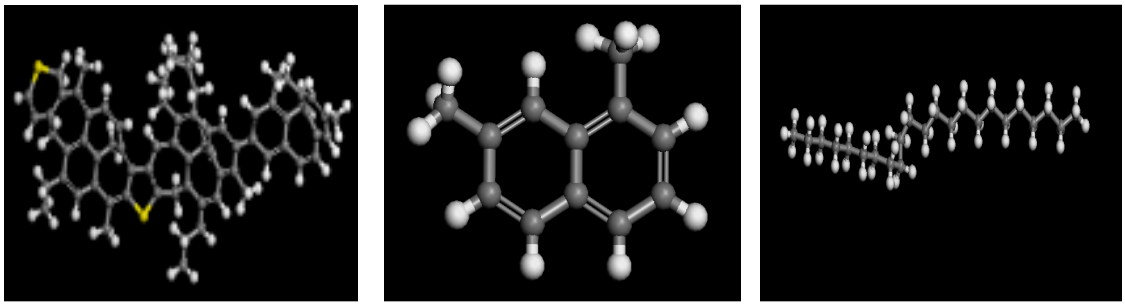

Figure 14: (a) Asphaltene (b) 1-7, di Methyl Naphthalene (c) n-Docosane

- Napthene Aromatics: These are mixed paraffin-napthene aromatics with traces of sulfur. In this research work, the napthene aromatics are represented by 1-7 di Methyl Naphthalene whose structure is as shown in Figure 14 (b).
- Saturates: saturates can be pure paraffin or pure napthene or mixed paraffin-napthene. In this research work, saturates are assumed to be pure paraffin and is represented by n-Docosane (n-$C_{22}H_{46}$). The structure of n-Docosane is as shown in Figure 14 (c).

The typical structures used to represent asphaltene, napthene and saturates were obtained from the literature *(17)*.

II. Minimization of Representative Molecules:

Molecules after sketching will be in random conformations and in general will have high energy configurations. Therefore it is desirable to minimize each sketched molecule before constructing an ensemble of molecules that represent the bulk. Figure 15 shows screen shots from the "Materials Studio" software from the minimization process.

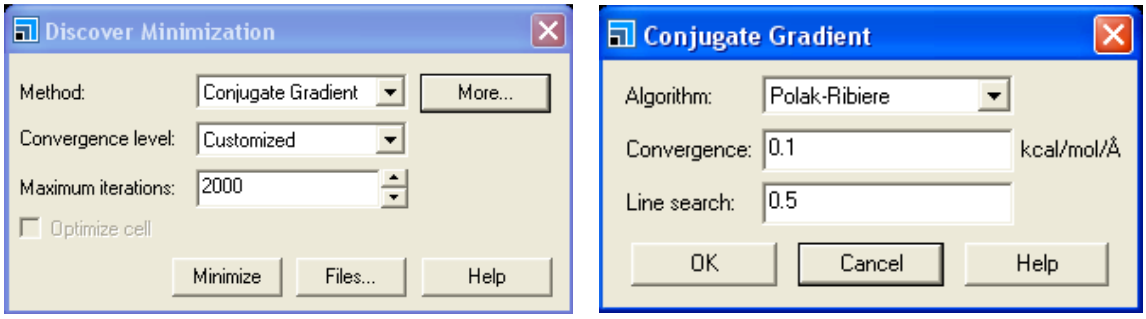

Figure 15: Screenshots of the Minimization Process

Conjugate gradient method with medium convergence level up to 2000 iterations was selected for the minimization. Figure 16 shows the results of the minimization step. Potential energy of the asphaltene molecule was reduced from around 1750 k Cal/mole to around 1200 k Cal/mole. Although the maximum allowed iterations were set as 2000, the minimization process typically stopped at around 1500 iterations as the convergence limit of 0.1 k Cal/mol/A^0 was reached.

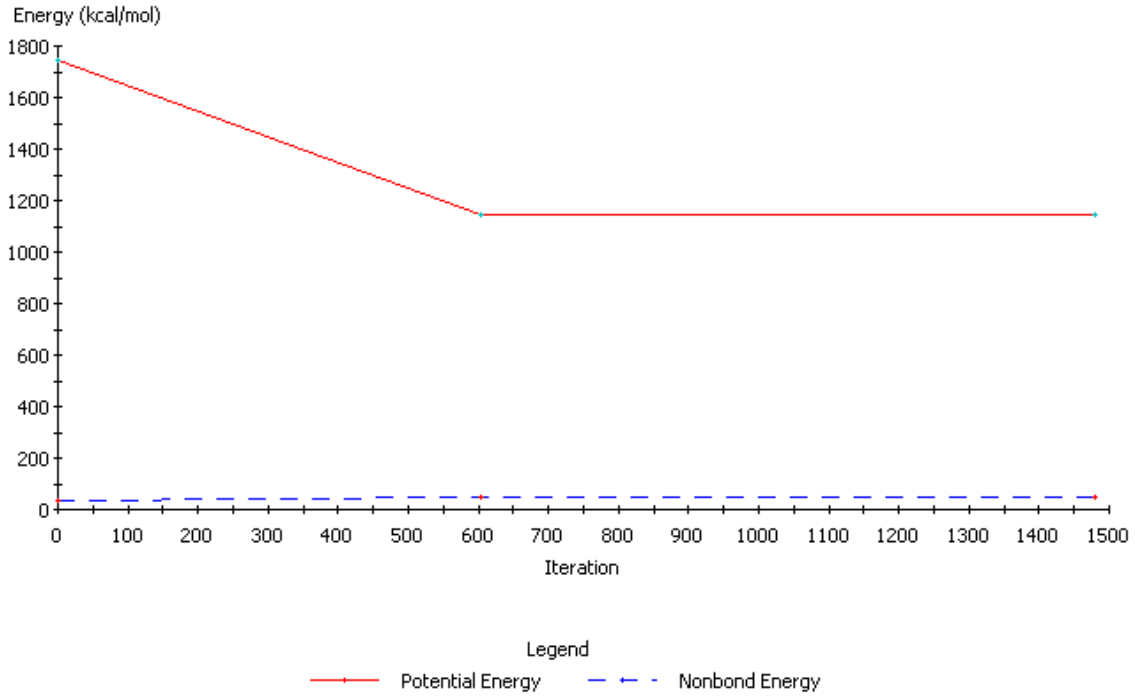

Figure 16: Energy Minimization of Asphaltene

III. Construction of Amorphous Cells:

An amorphous cell can be considered as an ensemble of molecules that are representative of the properties of the bulk binder. As discussed before, two approaches were used to input molecular structure and composition of asphalt molecules for the simulation. In one approach average molecular structure for SHRP binders obtained using NMR spectra were used as an input. In this case the unit amorphous cell was constructed using 10 average molecules per cell. In the second case, constituent and typical asphaltene, napthene, and saturate molecules were used to represent a hypothetical asphalt binder. In this case, the unit amorphous cell was constructed based on the assumed weight proportions of each constituent while keeping the total molecular weight constant, close to 4500 amu. The value of 4500 amu was selected as this was the

minimum possible weight while maintaining the assumed weight proportions. The other parameters used while constructing the amorphous cell were: Target Density = 1 g/cc; Temperature = 298 K; Dynamics Duration = 1 ps. The screen shot of the amorphous cell construction process is shown in Figure 17.

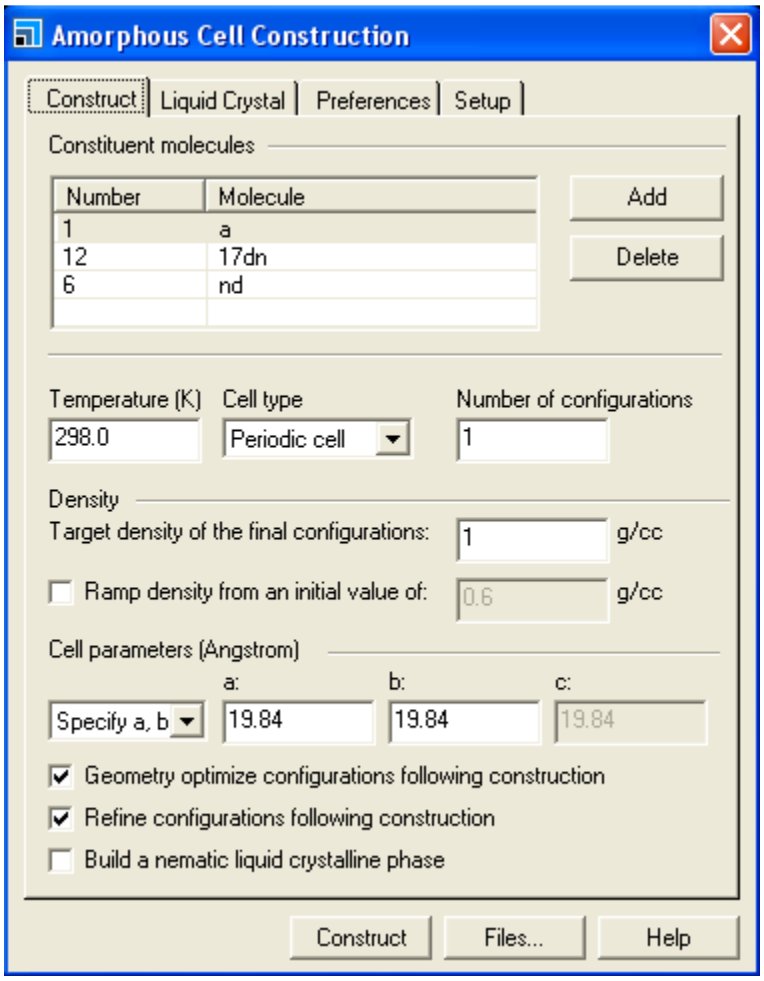

Figure 17: Amorphous Cell Construction Specifications

It can be seen from the above figure that a unit amorphous cell of an asphalt binder contains one asphaltene molecule, twelve di-methyl naphthalene molecules and six n-

docosane molecules. The number of molecules per cell is based on the design weight proportions, 20 % -20 % - 60 %. The constructed unit cell is as shown in Figure 18.

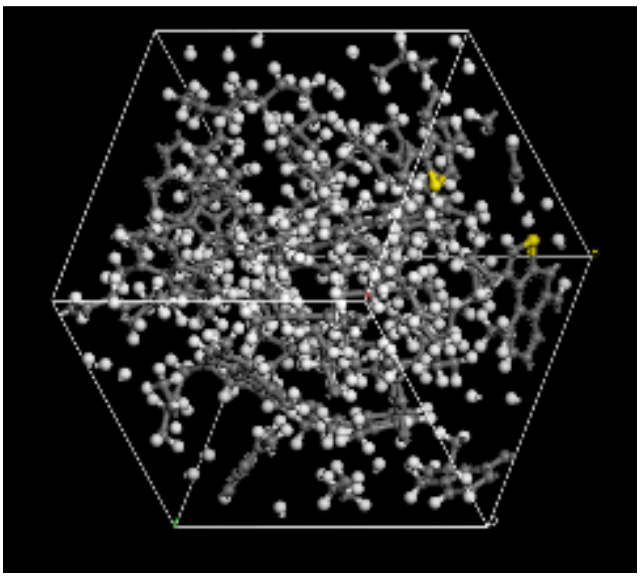

Figure 18: Asphalt Unit Cell

IV. Minimization:

The constructed amorphous cell is subjected to minimization. The parameters used for minimization were the same as that used in step II. The results of the minimization process are shown in Figure 19.

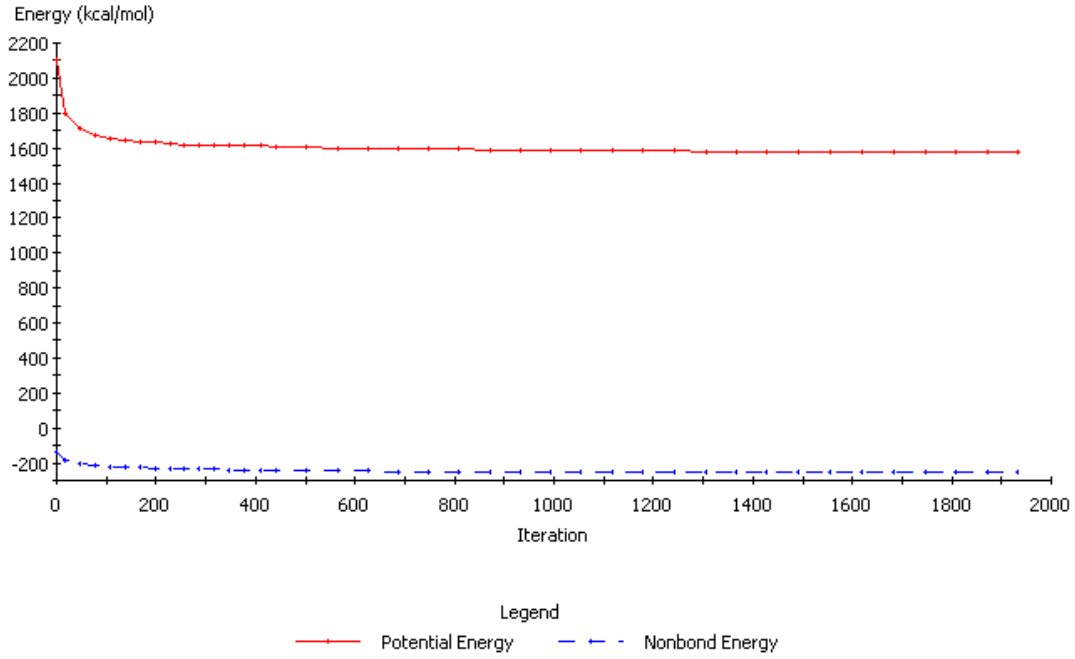

Figure 19: Minimization of Amorphous Cell

V. Dynamics:

Next step after the minimization was to conduct molecular dynamics. A screenshot of the dynamics process is as shown in Figure 20. As it can be seen from the details of Figure 20, the dynamics process outputs 50 frames. The main product of a dynamics run is a trajectory file that records the atomic configuration, atomic velocities and other information for these 50 frames that can be analyzed subsequently. Figure 21 illustrates the potential energy details for these 50 frames.

VI. Minimization and determination of bulk potential energy:

The frame with minimum energy (4th frame in the case of figure 21) was taken and minimized for energy. The potential energy after the minimization was recorded as 1569 kcal/mol.

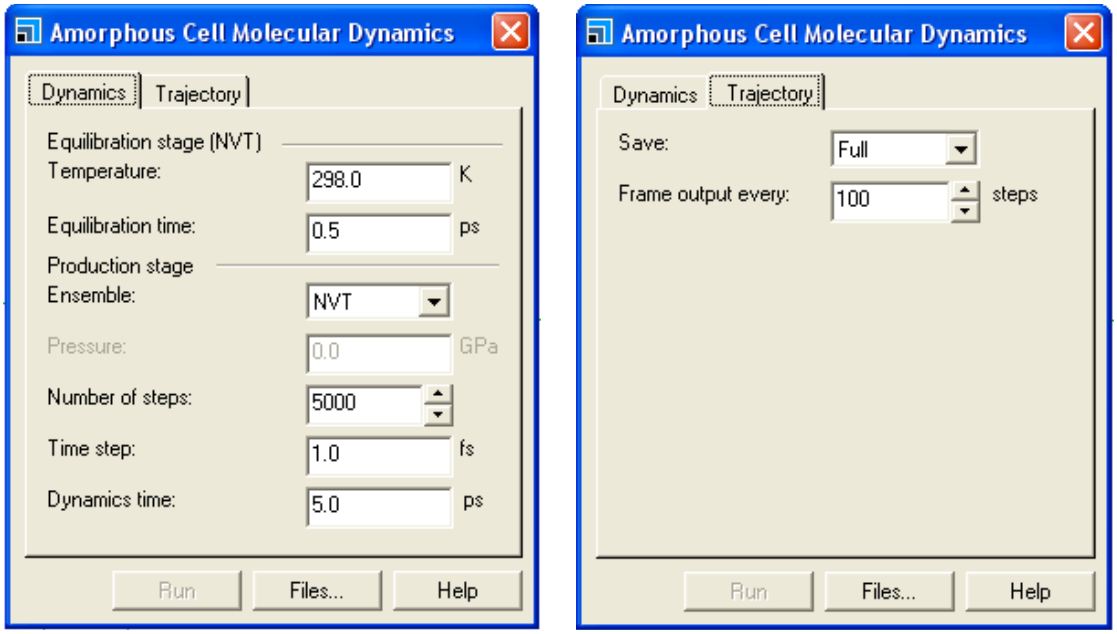

Figure 20: Molecular Dynamics

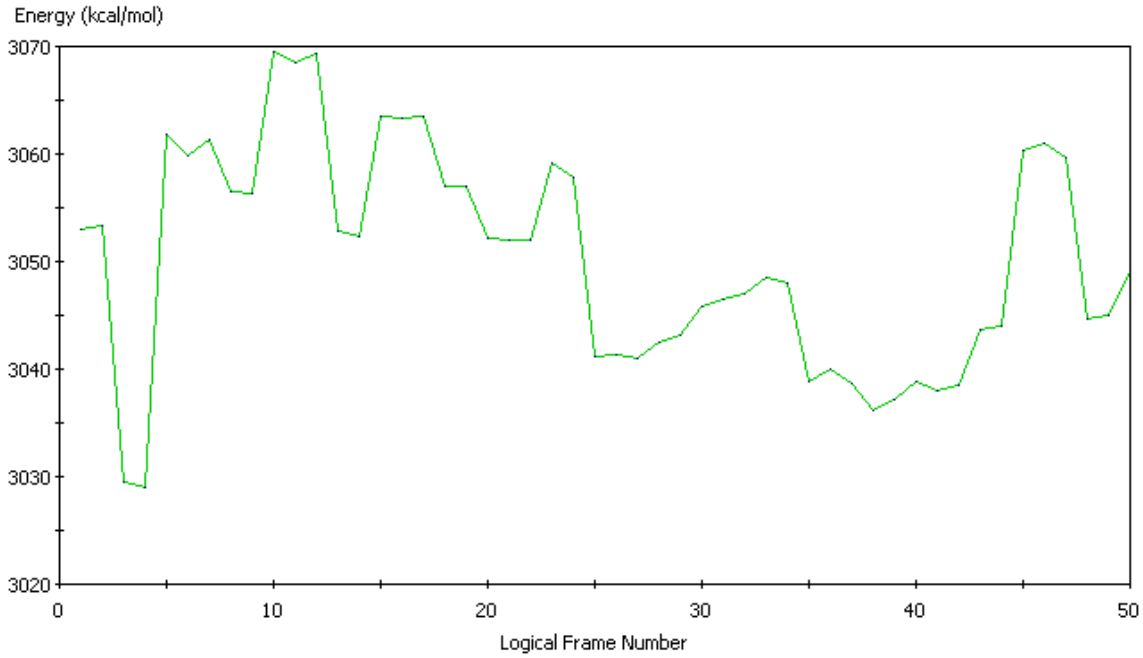

Figure 21: Total Energy vs. Logical Frame Number

VII. Formation of layers by Adding a Vacuum Pad of 50 A^0:

Surfaces were created by adding a vacuum pad of 50 A^0 in depth to the unit cell. The structure of unit cell after the addition of vacuum pad is as shown in Figure 22. Formation of layers can be clearly seen by expanding the view to multiple unit cells (bulk structure view) as shown in Figure 23 and Figure 24.

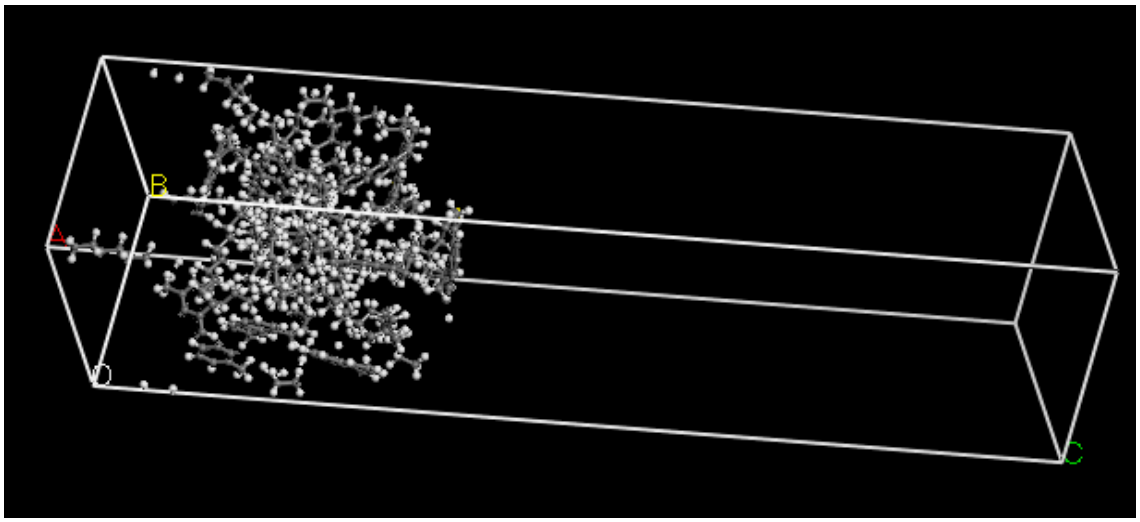

Figure 22: Unit Cell after the Addition of Vacuum Pad

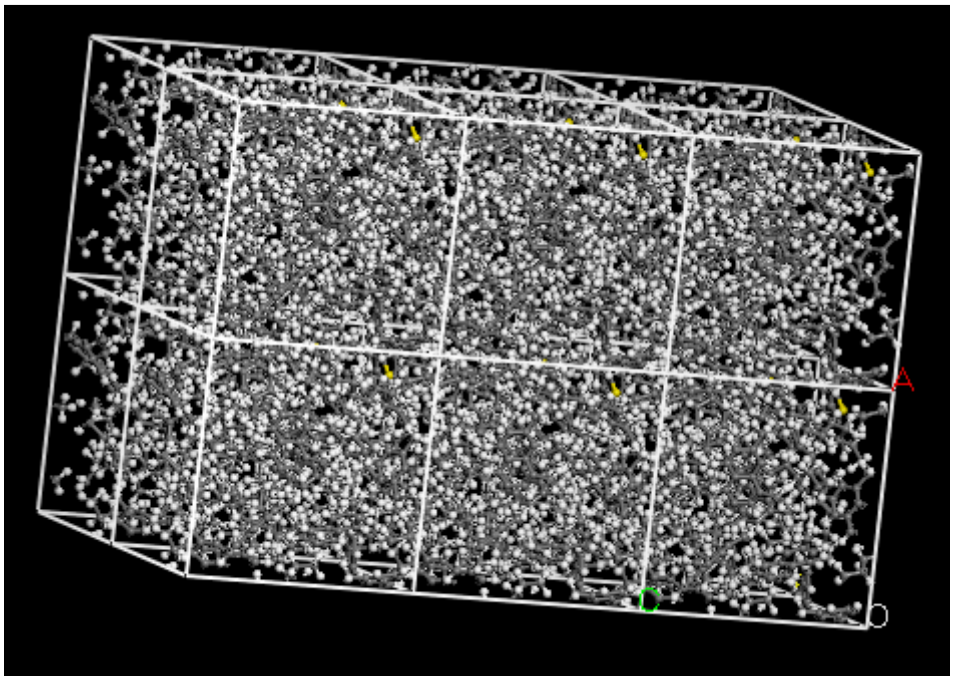

Figure 23: View of Multiple Unit Cells before the Addition of Vacuum Pad

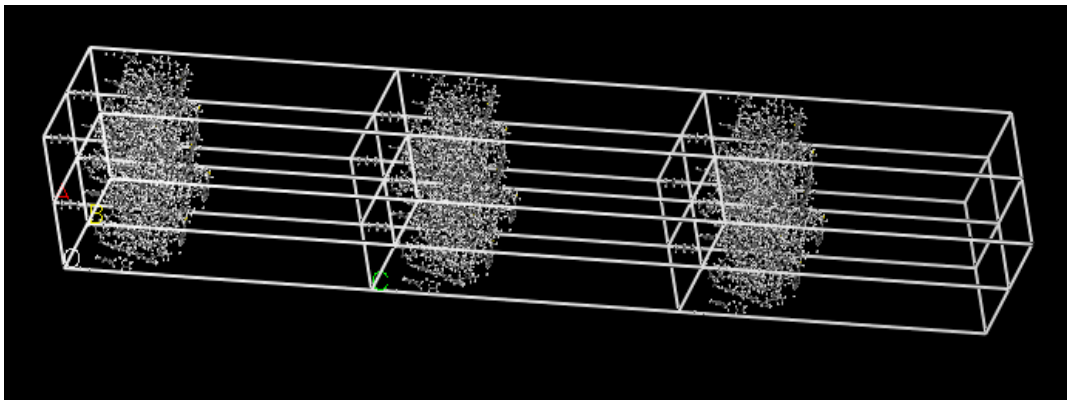

Figure 24: View of Multiple Unit Cells after the Addition of Vacuum Pad

VIII. Minimization of Layers:

The layers were minimized after their construction. The same minimization process as earlier was used.

IX. Dynamics of the Layer:

The minimized layered structure was subjected to molecular dynamics. The corresponding energy vs. frame number data for the layered structure shown in Figure 24 is as shown in Figure 25.

X. Minimization and Determination of Layer Potential Energy:

Frame 4 was selected for minimization and potential energy was recorded after the minimization process. The value of potential energy was 1689 kcal/mol.

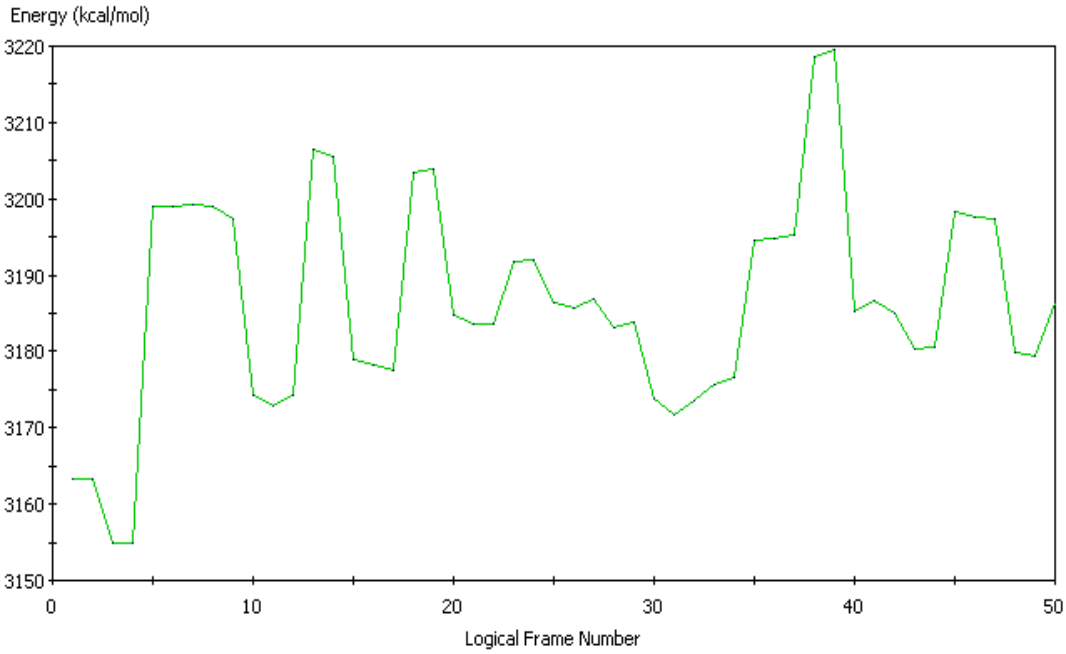

Figure 25: Energy vs. Frame Number Graph for Layered Structure

XI. Calculation of Surface Energies:

Surface energy values are calculated based on bulk and layer potential energies (15-17). The potential per mole before the formation of layers is 1569 kcal and the value after the formation of layers was 1689 kcal. The difference in these two energies is equal to the amount of residual potential energy stored on creating the surface. Surface energy is the amount of energy required for the creation of unit surface area, (Equation 1). Thus from the energy states of the bulk and layer the surface energy can be estimated as;

$$\frac{(1689 - 1569)\ \text{kcal/mole}}{[2 * \{(19.84)^2\ (\text{A}^\circ)^2\}]/\text{molecule}}$$

$$= \frac{(1689-1569)\ \text{kcal}}{2*\{(19.84)^2\ (\text{A}^\circ)^2\}*\text{Avogadro Constant}} \approx 106\ \text{ergs per sq. cm}$$

4.3.2 Method to Determine Diffusion-Coefficient

The trajectory file, which is the output of dynamics process, records the atomic configuration, atomic velocities and other information. This information can be used track the motion of molecules. In other words the diffusivity coefficient of molecules can be determined using this information. Also the diffusion behavior of molecules that reside within the bulk of the material bulk diffusivity is different from the diffusion of molecules that reside at the surface of the material i.e. surface diffusivity. Coefficients for both these diffusions can be calculated using this method. Step wise procedure to determine the diffusion coefficients are as follows:

I to IV: Steps I through IV are the same as those used to determine the surface free energy

V: Divide the unit cell, after minimization, into three equal parts i.e. three subsets. This division is used to calculate the diffusion coefficients for each subset separately. In this context division does entail any physical division of the amorphous cell, it is demarcation of the three subsets in the complete unit cell. Figure 26 illustrates a typical unit cell depicting the three sections.

VI. Dynamics:

After marking the subsections in the unit cell, it is subjected to dynamics. After the dynamics, mean square displacement (MSD) values were calculated for each of the subsection. A typical example of the data obtained for the middle section (Section 2) is as shown in Figure 27.

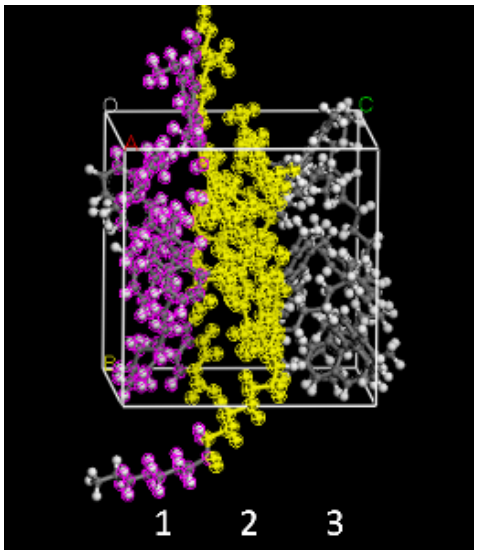

Figure 26: Unit Cell with Three Subsections

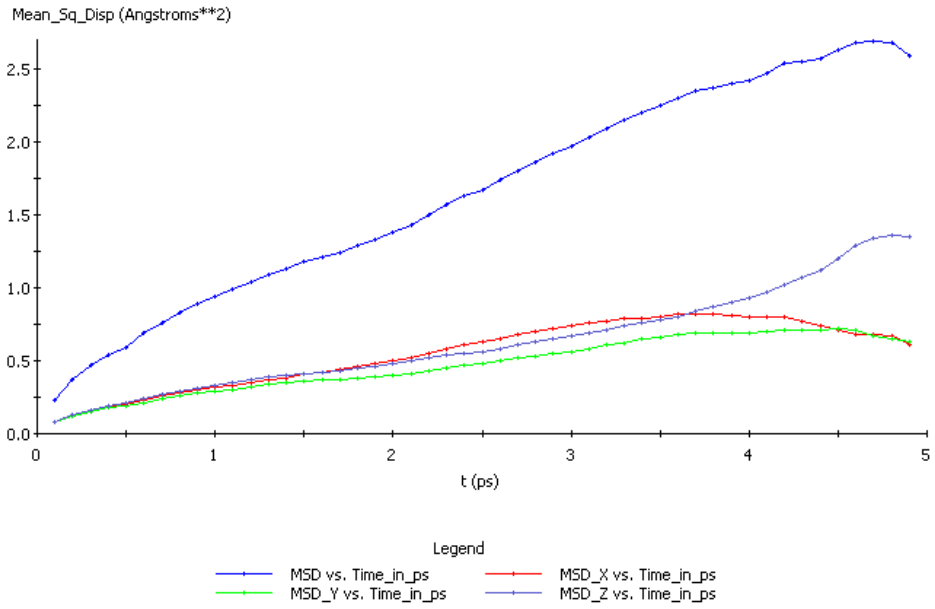

Figure 27: Mean Square Displacement Value for the Middle Section of the Unit Cell

Since MSD values represent the motion of the molecules these values can be used to determine the self diffusion coefficient. Figure 27 shows the average MSD value of all the molecules in a unit amorphous cell illustrated in Figure 26. In Figure 27, the bottom three curves illustrate the MSD values in the direction of three different Cartesian coordinates. The top curve is the resultant MSD. The data from figure 27 can be transferred to an Excel sheet. After transferring the data to a spread sheet, the MSD values are plotted against time (Figure 28).

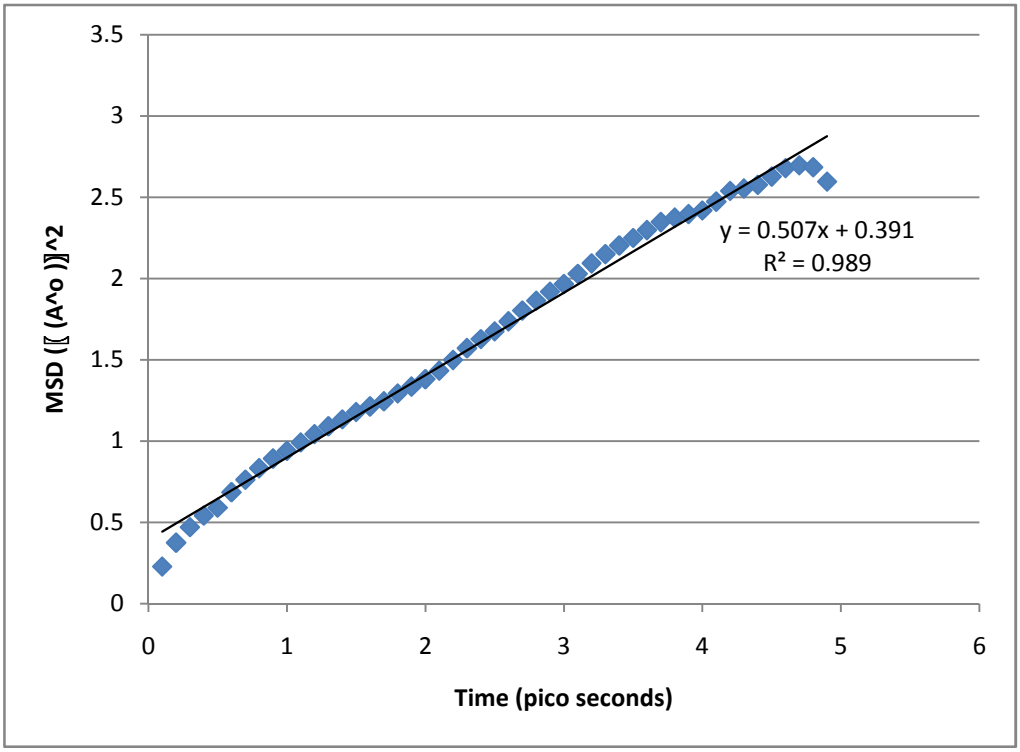

Figure 28: MSD with Respect to Time

The diffusion coefficient value is equal to one sixth of the slope (*15)*. For example, for the results illustrated in Figure 28 the molecular diffusivity was determined as follows:

$$\approx \frac{0.507}{6} \, (\mathrm{A^o})^2/_{\mathrm{ps}} \quad \approx 84 * 10^{-5} \, \mathrm{mm}^2/_{\mathrm{sec}}.$$

VII: In order to calculate the diffusion coefficients for the interface layer, a layered structure is created from the bulk asphalt, Figure 29. The layered structures are created such that the two asphalt surfaces are just in contact with each other. Here L1, L2 and L3 represent the corresponding subsets (1, 2 and 3) of selected molecules from the unit cell before formation of the layers.

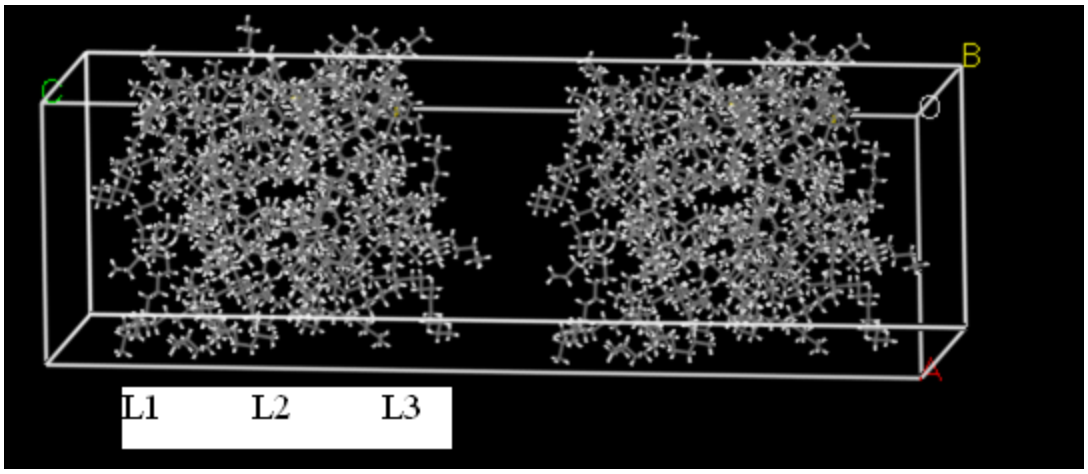

Figure 29: Layered Structure with Two Surfaces Just in Contact (before Dynamics).

VIII: Above layered structure is subjected to dynamics. The output of the layered structure after the diffusion is as shown in Figure 30.

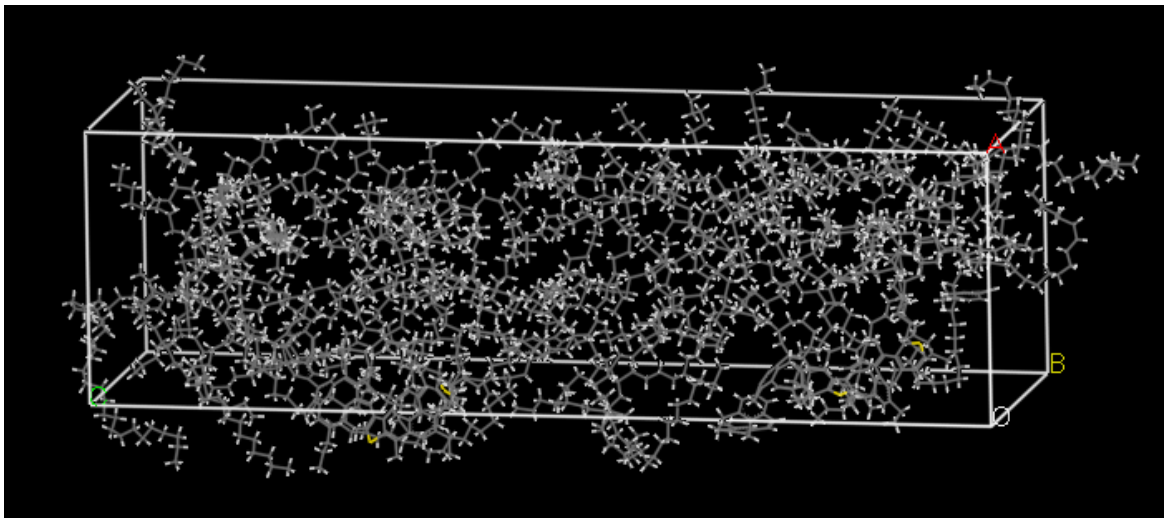

Figure 30: Layered Structure After Dynamics

IX: Now the MSD values for all the three sets (L1, L2 and L3) of the layered structure are calculated as explained previously in step 3. The diffusion coefficient values calculated from the MSD values of L1 and L3 are the interface diffusion coefficient values. The two values are calculated to be $\approx 130 * 10^{-5}\,\mathrm{mm^2/_{sec}}$ and $\approx 141 * 10^{-5}\,\mathrm{mm^2/_{sec}}$ respectively.

4.4 Results and Conclusions

4.4.1 Surface Energy Values

Surface energy values for asphalt binders AAB, AAD, AAM, AAF and AAG were determined using molecular simulation (as described in section 4.3.1). SHRP average molecules were used to represent the molecular structure for each asphalt binders. The surface energy values are compared with the experimental surface energy values from the literature *(16)*, Figure 31.

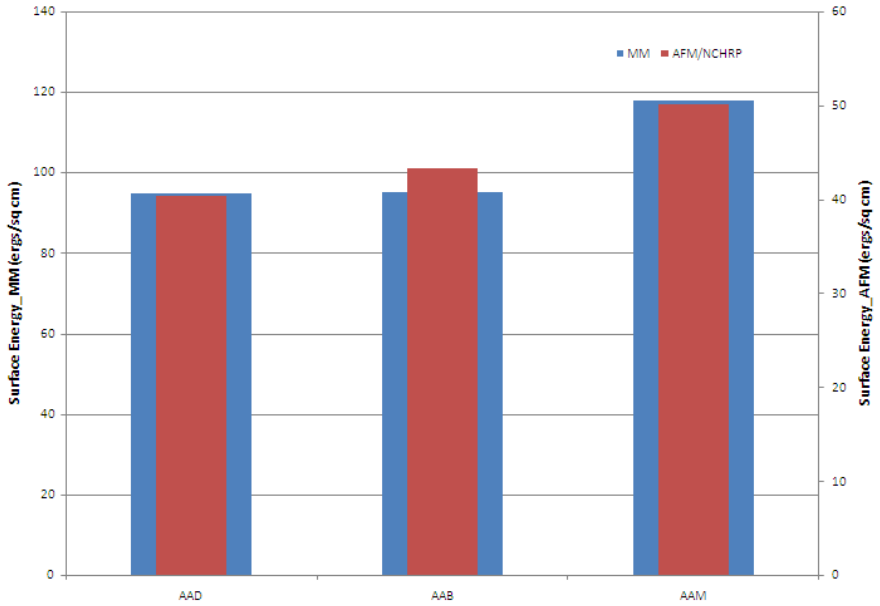

Figure 31: Comparison of Surface Energy Values Calculated Using Molecular Modeling Analysis with That of Values Calculated Using AFM Method

There seems to be a good agreement in the rank order between the experimental values and the values determined using molecular simulation. Though the absolute values do not coincide, they follow a similar trend. It is also assumed that the surface energy affects the healing of asphalt at initial stages and hence there expected to be a relation between surface energy values and short term healing index rates. Lytton et al. (REF) report the relative short term healing characteristics for different SHRP asphalt binders using mechanical tests. In their work the propensity for short term healing for different asphalt binders was quantified using a short term healing index. The short term healing index for different SHRP binders reported by Lytton et al. was compared to the surface free energy for these binders determined using the molecular simulations *(17).* There

seems to be a good agreement between the surface energy values and short term healing index rates, Figure 32.

Figure 32: Comparison of SE Values Calculated Using MM Analysis with Short Term Healing Index Rates

4.4.2 Diffusion Coefficient Values

Bulk (self) and surface diffusion coefficients for various SHRP binders were calculated for the SHRP binders using the method described in sections 4.3.2. As expected, the surface diffusion coefficients are much higher than the bulk diffusion coefficients. Figure 23 (gourps 1, 2, and 3) illustrates the subset of molecules from a bulk amorphous cell . Thus the corresponding diffusion coefficients values shown in Figure 33 (groups 1,2, and 3) represent the self diffusion coefficient values. The gourps identified as L1, L2 and L3 in Figure 33 are similar to groups 1,2 and 3 respectively, except that these are for a layered system . Therefore groups L1 and L3 represent molecules at the interface.

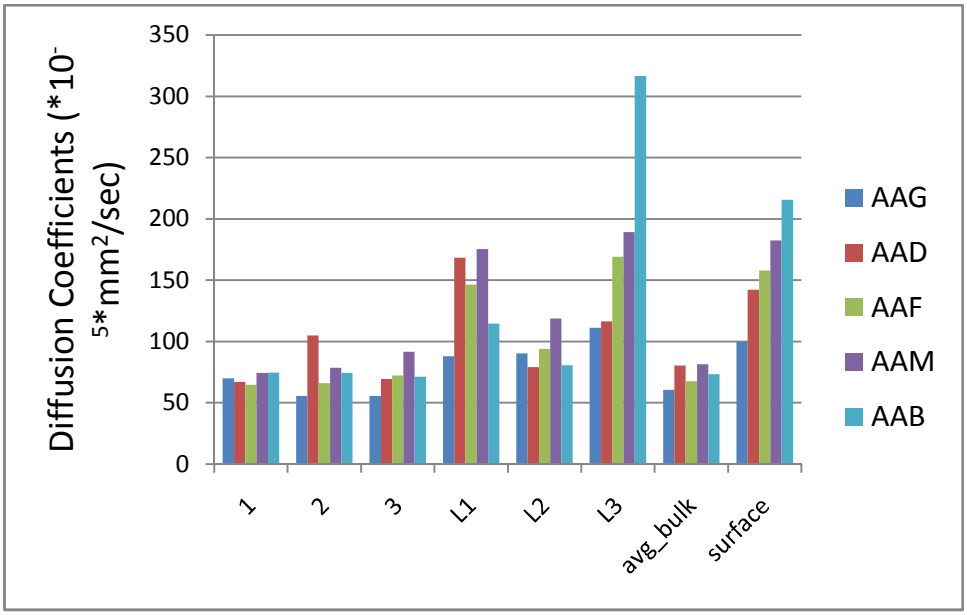

Figure 33: Diffusion Coefficient Values

The group marked as avg_bulk represents the average values of the three subgroups in bulk i.e. 1, 2 and 3. Diffusion Coefficient values marked as surface represents the average values of the two groups of molecules at the surface, L1 and L3. As expected, there is not much increase in the molecular diffusion coefficient for the group of molecules that are in the bulk of the system irrespective of the fact whether the molecules belong to the bulk of a continuous system or a layered system. From the figure it can also be seen that the surface diffusion coefficients are of the order AAG>AAD>AAF>AAM>AAB. This suggests that for the portion of healing mechanism most influenced by molecular diffusion AAG will be more effective than AAB. However, these results must be interpreted with caution since the overall healing rate is a function of mechanical and viscoelastic properties of the binder, surface free energy, and molecular diffusivity. Furthermore, the results from this analysis are based

on the use of a single average molecular structure that might not ideally represent the behavior of an ensemble of different molecules.

4.4.3 Parametric Analysis

Another objective of this research was to determine the influence of molecular morphology on properties such as surface free energy and molecular diffusivity. These properties are related to the rate of healing for different asphalt binders. In this task, diffusion-coefficients for different hypothetical asphalt binder systems were calculated by altering the proportion of its constituent molecules. Following proportions of Asphaltene-Napthene Aromatic-Saturates were evaluated: 20-20-60, 20-40-40 and 20-60-40. It was observed the higher the percentage of saturates, higher the diffusion-coefficient values, Figure 34.

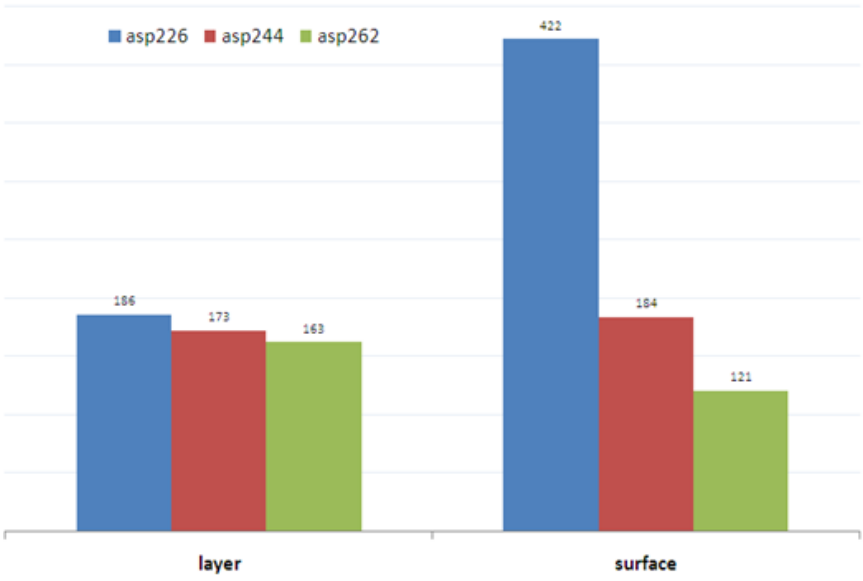

Figure 34: Parametric Analysis – Diffusion Coefficient vs. Saturate Percentage

In figure 34 the notation asp226 means asphalt with 20% asphaltenes, 20% napthene aromatics and 60% saturates, similarly asp 244 and 262. “Layer” denotes the diffusion coefficient of the total layer where as the “surface” denotes the diffusion coefficient of surface layer. Units of diffusion coefficients are ($*10^{-5}$ mm^2/sec).

5. SUMMARY AND CONCLUSIONS

5.1 DSR Method

Significant evidence exists in the literature that healing has a substantial effect on the performance of asphalt mixtures and consequently on the serviceable life of asphalt pavements. The incorporation of the healing mechanism in tandem with the crack growth mechanism is necessary for comprehensive modeling of the fatigue or fracture processes in asphalt mixtures. This thesis presents a new test method using the Dynamic Shear Rheometer to obtain some of the material properties related to the healing mechanism. A characteristic healing equation (Equation 6) was developed based on Schapery's wetting theory, Wool & O' Connors' intrinsic healing theory combined with theory of 'kinetics in phase transformation in solids'. Test results obtained using the DSR were used to determine the parameters for intrinsic healing for different asphalt binders (equation 6).

Basically shear modulus values for asphalt binders as they heal with respect to time are determined using DSR experiment. These shear modulus values are used to determine the percentage healing function R(t) which in turn is used to determine the parameters (R_0, p, q and r) of the characteristic healing function. 'R_o' represents the instantaneous healing nature of the binders and hence the effect of this parameter on the characteristic equation is analogous to the effect of surface energy on actual healing. The values of R_0 are calculated for three different types of binders; AAM, AAD and ABD. These values are compared with the surface energy values (taken from literature) of corresponding asphalt binders. Results from limited tests indicate that the rank order for

R_0 that corresponds to instantaneous healing of wetted surface is the same as work of cohesion obtained from surface energy measurements. Though the values are not exactly matching in terms of magnitude, they are proportional which means that the R_0 values determined using this test method can be used to predict the relative healing nature of the asphalt binders. Thus, using this test method one can tell which is better healer among the given asphalt binders. Not only that, the test results can also be used to rank the binders on its own scale.

5.1.1Scope for Future Work

- All the tests in this research were conducted at room temperature but the healing characteristics are highly temperature dependent. Therefore, it is important to extend this test procedure to different temperatures.
- The sample preparation techniques must be refined to accommodate the effect from the edges of the specimen on the measured values.
- Future work must also consider establishing a relationship between the DSR results and molecular modeling tools demonstrated in this research work.

5.2 Molecular Modeling

A protocol based on molecular modeling techniques was developed to determine the surface energy and molecular diffusion coefficients of asphalt binders. The accuracy of surface energy or diffusion coefficient values computed using the molecular modeling techniques is highly dependent on the accuracy of the molecular structure and composition used to represent a particular asphalt binder. With the present available

technology, it is not possible to determine the exact molecular structure and composition of asphalt binders. However, instead of trying to determine the absolute values of surface energy or diffusion coefficients, the focus of this research was to evaluate the trends in these values based on changes in the chemical makeup of asphalt binders. The surface energy values calculated using this method are compared with those values obtained from literature. The values seem to be agreeing well in terms of proportionality. Thus this method can be used to compare the surface energies of asphalt binders. From the diffusion coefficient values calculated using this test method it is observed that the molecules at interface diffuse faster than the molecules at bulk. Thus, interfacial diffusion coefficient may be the better parameter than self diffusion coefficient for estimating the healing in binders. The test method can be used to compare or determine the diffusion coefficients of asphalt binders. The main conclusions of this research work on molecular modeling are:

- Surface free energy computed using the MM techniques with average NMR based molecular structures:
  - ranked similar to values obtained from AFM techniques
  - ranked similar to short term healing index for SHRP binders
- Diffusivity of molecules at the interface was higher than diffusivity of molecules in the bulk
- It is recommended that due consideration to the above difference must be placed in modeling of healing mechanism

- MM demonstrates that higher percentage of saturates (longer chains) results in higher diffusivity and consequently better healing characteristics. This reinforces the conclusions drawn from an earlier study using FTIR (Little, Kim et al.)
- Percentage of saturates has much more impact on diffusivity at interface (related to healing of cracks) than self diffusivity

5.2.1 Scope for Future Work

Following is the list of few main areas where the test method can be improved by doing further work:

- Due to the time constraints of the project, the duration of dynamics used in this project is just 5 seconds. This should be increased largely to get reliable results.
- The accuracy of results from this analysis is dependent on the accuracy of the chemical structures used to represent the asphalt binder in simulation. Therefore, it is important to continually update the the molecular structures that are used in these simulations. Also in this analysis, polar aromatics were not considered. These should also should be included by determining an appropriate representative molecular structure.
- Force filed is a key element in the whole analysis. Though the force filed used in this method is the most advanced to be used for asphalt compounds, it is desirable that a force filed be designed especially for asphalt research.

REFERENCES

1) Wool, R. P., and K.M. O'Connor. A Theory of Crack Healing in Polymers. *Journal of Applied Physics.* Vol. 52, 1981, pp. 5953-5963.

2) Little, D. N., Lytton, R. L., Williams, A. D., and Chen, C. W. *Micro Damage Healing in Asphalt and Asphalt Concrete, Volume I: Micro Damage and Micro Damage Healing.* Project Summary Report, FHWA-RD-98-14, Texas Transportation Institute, College Station, TX, 2001.

3) Kim, Y. R., Little, D. N., and Lytton, R. L. Fatigue and Healing Characterization of Asphalt Mixes. *Journal of Materials in Civil Engineering (ASCE)*, Vol. 15, 2003b, pp. 75-83.

4) Carpenter, S. H., and Shen, S. A Dissipated Energy Approach to Study HMA Healing in Fatigue. In *Transportation Research Record: Journal of the Transportation Research Board, No. 1970,* Transportation Research Board of the National Academies, Washington, D.C., 2006, pp. 178 to 185.

5) Kim, B., and Roque, R. Evaluation of Healing Property of Asphalt Mixture. In *Transportation Research Record: Journal of the Transportation Research Board, No. 1970* Transportation Research Board of the National Academies, Washington, D.C., 2006, pp. 84-91.

6) Maillard, S., de La Roche, C., Hammoum, F., Gaillet, L., and Such, C. Experimental Investigation of Fracture and Healing at Pseudo-Contact of Two Aggregates. *3rd Euroasphalt and Eurobitume Congress,* Vienna, 2002.

7) Bhairampally, R. K., Lytton, R. L., and Little, D. N. Numerical and Graphical Method to Assess Permanent Deformation Potential for Repeated Compressive Loading of Asphalt Mixtures. In *Transportation Research Record: Journal of the Transportation Research Board, No. 1723*, Transportation Research Board of the National Academies, Washington, D.C., 2000, pp. 150-158.

8) Song, I., Little, D. N., Masad, E., and Lytton, R. Comprehensive Evaluation of Damage in Asphalt Mastics Using X-Ray CT, Continuum Mechanics, and Micro-Mechanics. *Association of Asphalt Paving Technologists*, Vol. 74, 2005, pp. 885-920.

9) Williams, A. D., Little, D. N., Lytton, R. L., Kim, Y. R., and Kim, Y. *Microdamage Healing in Asphalt and Asphalt Concrete, Volume II: Laboratory and Field Testing to Assess and Evaluate Microdamage and Microdamage Healing.* FHWA-RD-98-142, Texas Transportation Institute, College Station, TX, 2001.

10) Nishizawa, T., Shimeno, S., and Sekiguchi, M. Fatigue Analysis of Asphalt Pavements with Thick Asphalt Mixture, Layer. *8th International Conference on Asphalt Pavements,* Seattle, WA, 1997, 969-976.

11) Little, D. N., and Bhasin, A. Exploring Mechanisms of Healing in Asphalt Mixtures and Quantifying its Impact. *Self Healing Materials,* S. van der Zwaag, ed., Springer, The Netherlands, 2007, pp. 205-218.

12) Robertson, R. Chemical Properties of Asphalts and Their Effects on Pavement Performance. In *Transportation Research Record: Journal of the Transportation Research Board, No. 499*, Transportation Research Board of the National Academies, Washington, D.C., 2000 pp 46p.

13) Storm, D. A., J. C. Edwards, S. J. DeCanio, and E. Y. Sheu. Molecular Representations of Ratawi and Alaska North Slope Asphaltenes Based on Liquid- and Solid-state NMR, *Energy & Fuels,* Vol. 8, 1994, pp. 561-566.

14) Jennings P.W., J. A. Pribanic, M.A. Desando, M.F. Raub, R. Moats, Smith, J A; Mendes, T M; McGrane, M ; Fanconi, B ; VanderHart, D L; Manders, W F. *Binder Characterization and Evaluation by Nuclear Magnetic Resonance Spectroscopy*. *SHRP-A-335,* Strategic Highway Research Program, National Research Council, Washington, D.C., 1993.

15) Deng. M., V.B.C. Tan, T.E. Tay. Atomistic Modeling: Interfacial Diffusion and Adhesion of Polycarbonate and Silanes. *Polymer,* Vol. 45, 2004, pp. 6399-6407.

16) Clancy, T.C., W.L. Mattice. Computer Simulation of Polyolefin Interfaces. *Comp and Theo Polymer Science,* Vol 9, 1999, pp. 262-270.

17) Greenfield, M.L., and L. Zhang. Analyzing Properties of Model Asphalts Using Molecular Simulation. *Energy and Fuels,* Vol. 21, No. 3, 2007, pp. 1712-1716.

18) Schapery, R. A. Non linear Fracture Analysis of Viscoelastic Composite Materials Based on a Generalized J Integral Theory. *Japan - U.S. Conference on Composite Materials: Mechanics, Mechanical Properties and Fabrication*, Tokyo, Japan, 1998, pp. 171-180.

19) Berger, L. L., and Kramer, E. J. Chain Disentanglement during High Temperature Crazing of Polystyrene. *Macromolecules*, Vol. 20, 1987, pp. 1980-1985.

20) Kim, Y., Little, D. N., and Lytton, R. L. Fatigue and Healing Characterization of

Asphalt Mixtures. *Journal of Materials in Civil Engineering (ASCE)*, Vol. 15, No.1, 2003, pp. 75-83.

21) Schapery, R. A. On the Mechanics of Crack Closing and Bonding in Linear Viscoelastic Media. *International Journal of Fracture*, Vol. 39, 1989, pp.163-189.

22) de Gennes, P. G. Reptation of a Polymer Chain in the Presence of Fixed Obstacles. *The Journal of Chemical Physics*, Vol. 55, No. 2, 1971, pp. 572-579.

23) Lytton, R. L., Chen, C. W., and Little, D. N. *Micro-Damage Healing in Asphalt and Asphalt Concrete, Volume III: A Micromechanics Fracture and Healing Model for Asphalt Concrete.* FHWA-RD-98-143, Texas Transportation Institute, College Station, TX, 2001.

24) Callister, W. D. J. *Materials Science and Engineering An Introduction*. John Wiley & Sons, NY, 2007.

25) Charati, S. G., and Stern, Diffusion of Gases in Silicone Polymers: Molecular Dynamics Simulations S A. *Macromolecules,* Vol. 31, 1998, pp. 5529-5538.

26) Little, D., and A. Bhasin. *Using Surface Energy Measurements to Select Materials for Asphalt Pavement.* NCHRP-104, Project 9-37, Texas Transportation Institute, College Station, TX, 2007.

27) Lytton, R. L. Characterizing Asphalt Pavements for Performance. In *Transportation Research Record: Journal of the Transportation Research Board,* 1723, Transportation Research Board of the National Academies, Washington, D.C., 2000, pp. 5-16.

APPENDIX 1

Average Molecular Structures of SHRP Core Asphalts

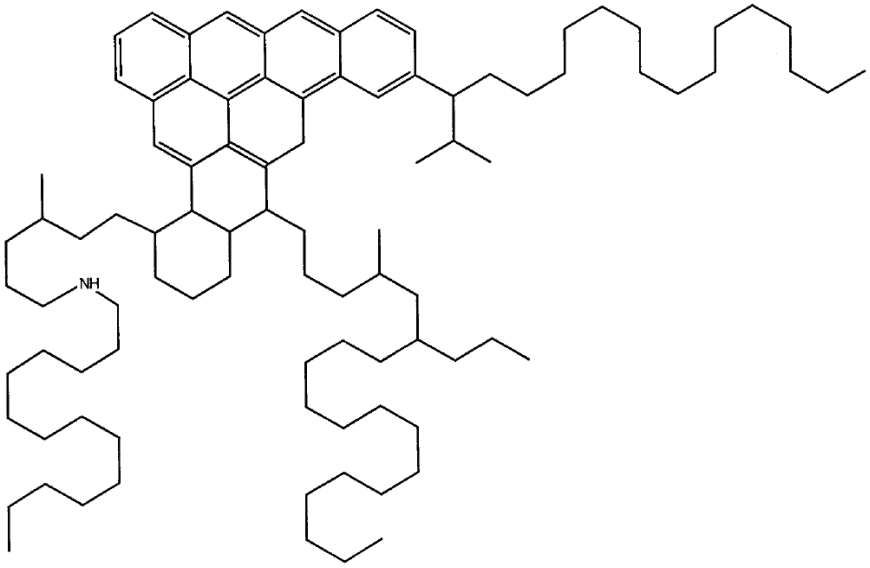

Figure 35: Average Molecular Structure of AAM

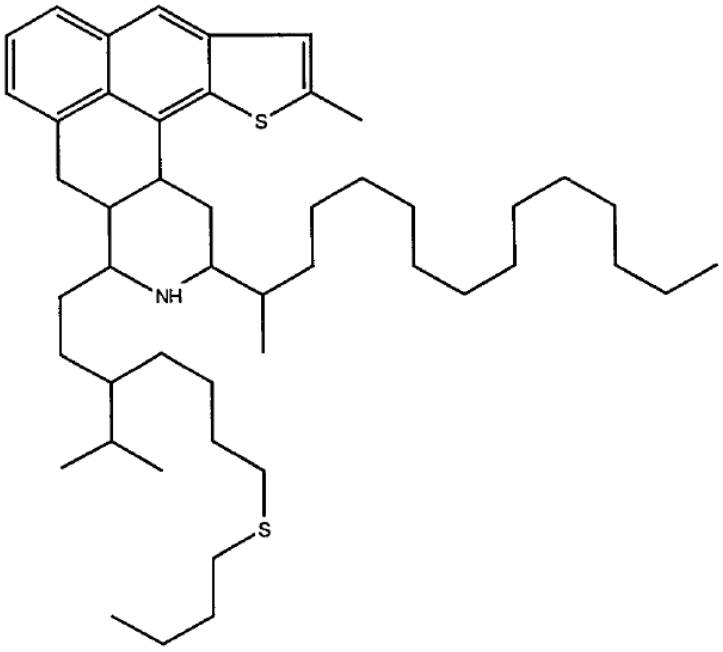

Figure 36: Average Molecular Structure of AAD

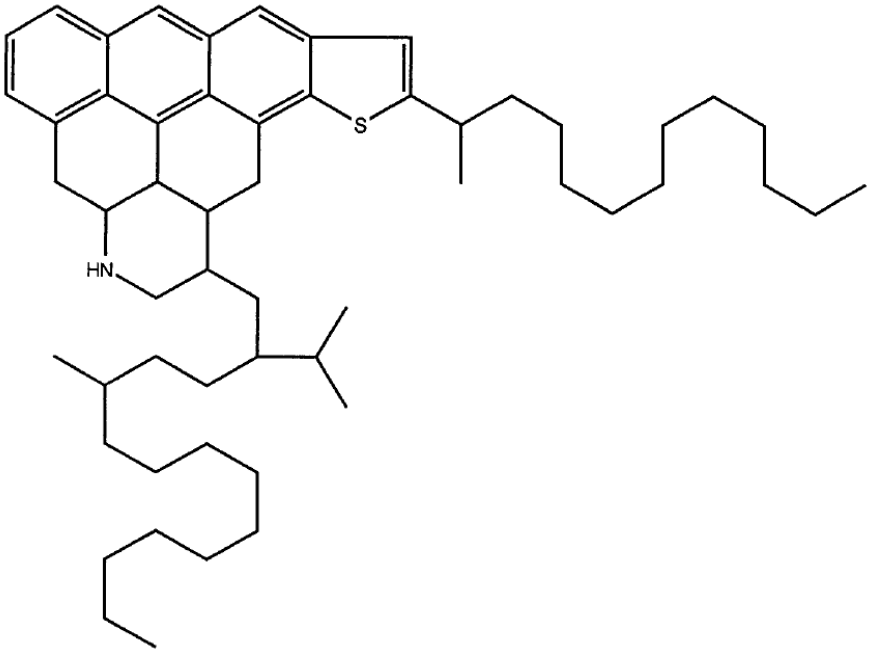

Figure 37: Average Molecular Structure of AAA -1

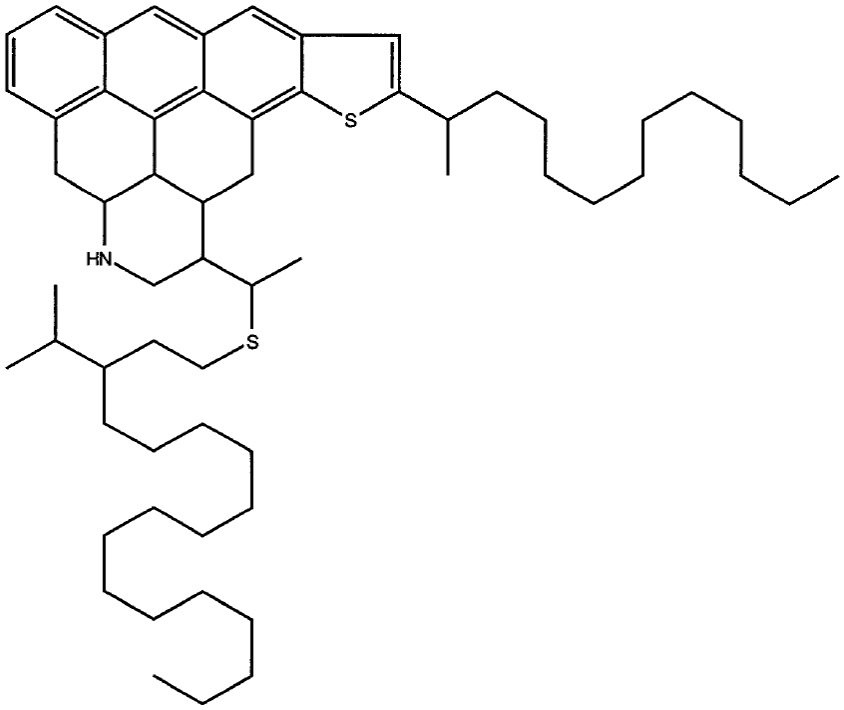

Figure 38: Average Molecular Structure of AAK-1

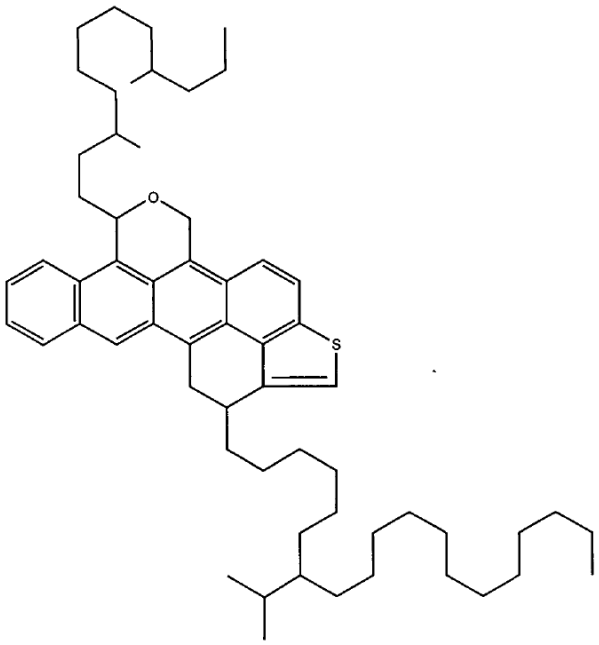

Figure 39: Average Molecular Structure of AAF-1

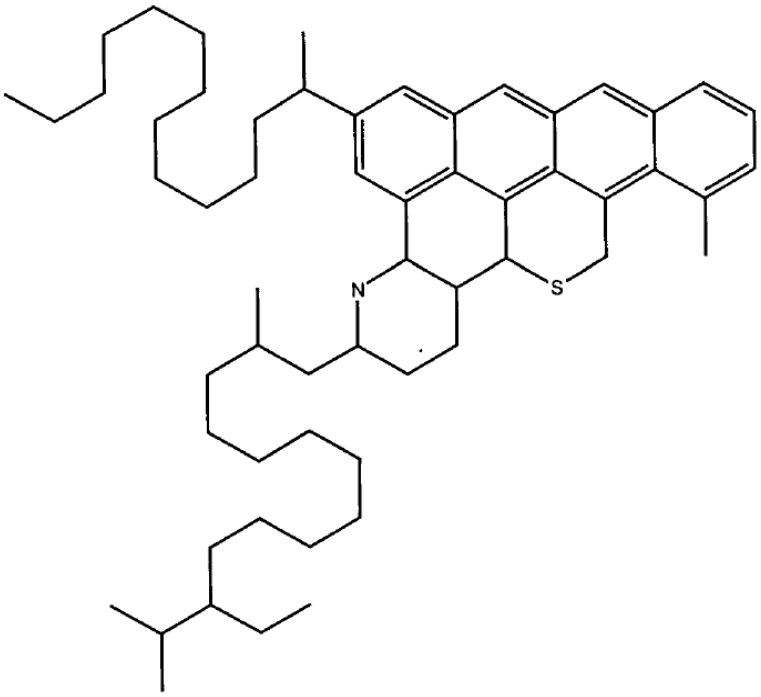

Figure 40: Average Molecular Structure of AAB-1

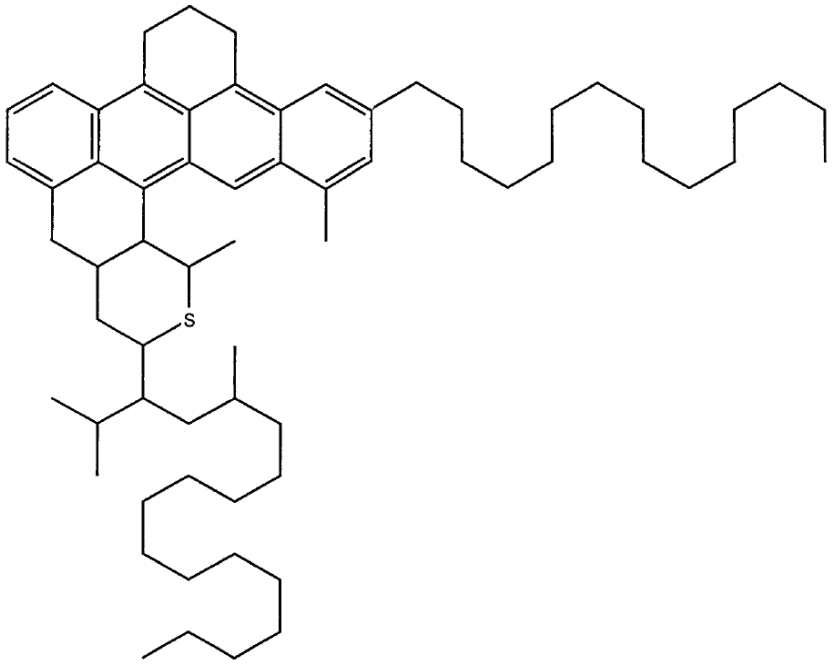

Figure 41: Average Molecular Structure of AAC-1

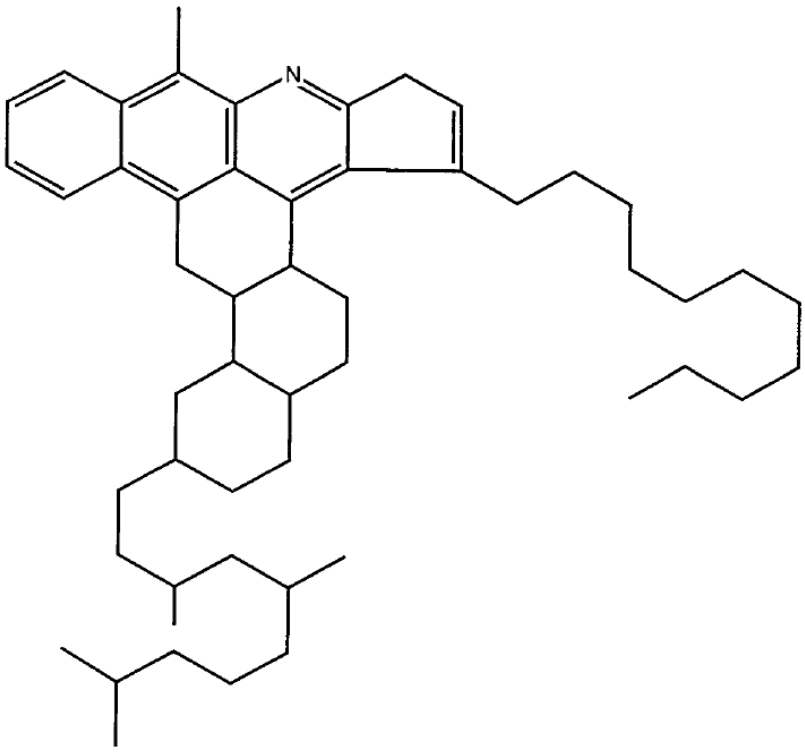

Figure 42: Average Molecular Structure of AAG-1

VITA

Name:	Ramamohan Reddy Bommavaram
Address: S/O:	Narayana Reddy Bommavaram Erracheruvu Palli, Tangutur (Post) Nandalur (Mandal), kadapa (District) Andhra Pradesh – 516151 India
Email Address:	rammohanreddy.b@gmail.com
Education:	B.Tech., Civil Engineering, Indian Institute of Technology – Madras, 2006 M.S., Civil Engineering, Texas A&M University, 2008